

*Midwest State's Regional Pooled Fund Research Program
Fiscal Year 1998-2000 (Year 9 & 10)
NDOR Research Project Number SPR-3(017)*

DEVELOPMENT OF A W-BEAM GUARDRAIL SYSTEM FOR USE ON A 2:1 SLOPE

Submitted by

Karla A. Polivka, B.S.M.E., E.I.T.
Research Associate Engineer

Dean L. Sicking, Ph.D., P.E.
Associate Professor and MwRSF Director

James C. Holloway, M.S.C.E., E.I.T.
Research Associate Engineer

Ronald K. Faller, Ph.D., P.E.
Research Assistant Professor

John R. Rohde, Ph.D., P.E.
Associate Professor

Eric A. Keller, B.S.M.E., E.I.T.
Research Associate Engineer

MIDWEST ROADSIDE SAFETY FACILITY

University of Nebraska-Lincoln
1901 "Y" Street, Building "C"
Lincoln, Nebraska 68588-0601
(402) 472-6864

Submitted to

MIDWEST STATE'S REGIONAL POOLED FUND PROGRAM

Nebraska Department of Roads
1500 Nebraska Highway 2
Lincoln, Nebraska 68502

MwRSF Research Report No. TRP-03-99-00

October 16, 2000

Technical Report Documentation Page

1. Report No. SPR-3(017)	2.	3. Recipient's Accession No.	
4. Title and Subtitle Development of a W-Beam Guardrail System for use on a 2:1 Slope		5. Report Date October 16, 2000	
		6.	
7. Author(s) Polivka, K.A., Faller, R.K., Sicking, D.L., Rohde, J.R., Holloway, J.C., and Keller, E.A.		8. Performing Organization Report No. TRP-03-99-00	
9. Performing Organization Name and Address Midwest Roadside Safety Facility (MwRSF) University of Nebraska-Lincoln 1901 Y St., Bldg. C Lincoln, NE 68588-0601		10. Project/Task/Work Unit No.	
		11. Contract © or Grant (G) No. SPR-3(017)	
12. Sponsoring Organization Name and Address Midwest States Regional Pooled Fund Program Nebraska Department of Roads 1500 Nebraska Highway 2 Lincoln, Nebraska 68502		13. Type of Report and Period Covered Final Report 1999-2000	
		14. Sponsoring Agency Code	
15. Supplementary Notes Prepared in cooperation with U.S. Department of Transportation, Federal Highway Administration			
16. Abstract (Limit: 200 words) <p>A W-beam guardrail system was developed and crash tested for use on a 2:1 foreslope. The guardrail design was constructed with 2.66-mm (12-gauge) thick W-beam rails totaling 53.34 m in length and incorporated a half-post spacing section of 17.15 m. The W-beam rail was supported by fifteen W152x13.4 by 1,829-mm long steel posts, spaced 1,905-mm on center, and nineteen W152x13.4 by 2,134-mm long steel posts, spaced 952.5-mm on center. Routed, 150x200x360 wood spacer blockouts were used to block the rail away from each post.</p> <p>The research study included bogie testing on steel posts placed in sloped fill and one full-scale vehicle crash test, using a ¾-ton pickup truck. The test, impacting at a speed of 100.7 km/hr and an angle of 28.5 degrees, was conducted and reported in accordance with the requirements specified in NCHRP Report No. 350, <i>Recommended Procedures for the Safety Performance Evaluation of Highway Features</i>. The safety performance of the W-beam barrier system was determined to be acceptable according to Test Level 3 (TL-3) of the NCHRP Report No. 350 criteria.</p>			
17. Document Analysis/Descriptors Highway Safety, Guardrail, Longitudinal Barrier, Roadside Slopes,		18. Availability Statement No restrictions. Document available from: National Technical Information Services, Springfield, Virginia 22161	
19. Security Class (this report) Unclassified	20. Security Class (this page) Unclassified	21. No. of Pages 95	22. Price

DISCLAIMER STATEMENT

The contents of this report reflect the views of the authors who are responsible for the facts and the accuracy of the data presented herein. The contents do not necessarily reflect the official views or policies of the State Highway Departments participating in the Midwest State's Regional Pooled Fund Research Program nor the Federal Highway Administration. This report does not constitute a standard, specification, or regulation.

ACKNOWLEDGMENTS

The authors wish to acknowledge several sources that made a contribution to this project: (1) the Midwest States Regional Pooled Fund Program funded by the Iowa Department of Transportation, Kansas Department of Transportation, Minnesota Department of Transportation, Missouri Department of Transportation, Nebraska Department of Roads, Ohio Department of Transportation, South Dakota Department of Transportation, and Wisconsin Department of Transportation for sponsoring this project; (2) MwRSF personnel for constructing the barrier and conducting the bogie and crash tests; and (3) the University of Nebraska-Lincoln for matching support.

A special thanks is also given to the following individuals who made a contribution to the completion of this research project.

Midwest Roadside Safety Facility

J.D. Reid, Ph.D., Associate Professor, Mechanical Engineering Department
R.W. Bielenberg, M.S.M.E., Research Associate Engineer
K.L. Krenk, B.S.M.A., Shop Manager
K.H. Addink, B.S.C.E., Research Associate Engineer
M.L. Hanau, Laboratory Mechanic I
D.M. McBride, Laboratory Mechanic I
Undergraduate and Graduate Assistants

Iowa Department of Transportation

David Little, P.E., Deputy Director, Engineering Division
Jay Chiglo, P.E., Methods Engineer

Kansas Department of Transportation

Ron Seitz, P.E., Road Design Squad Leader

Minnesota Department of Transportation

Ron Cassellius, Research Program Coordinator
Andrew Halverson, P.E., Assistant Design Standards Engineer

Missouri Department of Transportation

Vince Imhoff, P.E., Contract Administration Engineer
Tom Allen, P.E., Research and Development Engineer

Nebraska Department of Roads

Leona Kolbet, Research Coordinator
Ken Sieckmeyer, Transportation Planning Manager

Ohio Department of Transportation

Monique Evans, P.E., Roadway Standards Engineer

South Dakota Department of Transportation

David Huft, Research Engineer

Wisconsin Department of Transportation

Rory Rhinesmith, P.E., Chief Roadway Development Engineer
Peter Amakobe, Standards Development Engineer

Federal Highway Administration

Milo Cress, P.E., Nebraska Division Office
John Perry, P.E., Nebraska Division Office
Frank Rich, P.E., Nebraska Division Office

Dunlap Photography

James Dunlap, President and Owner

TABLE OF CONTENTS

	Page
TECHNICAL REPORT DOCUMENTATION PAGE	i
DISCLAIMER STATEMENT	ii
ACKNOWLEDGMENTS	iii
TABLE OF CONTENTS	v
List of Figures	vii
List of Tables	ix
1 INTRODUCTION	1
1.1 Problem Statement	1
1.2 Objective	1
1.3 Scope	2
2 LITERATURE REVIEW	3
3 TEST REQUIREMENTS AND EVALUATION CRITERIA	5
3.1 Test Requirements	5
3.2 Evaluation Criteria	5
4 DEVELOPMENTAL TESTING – BOGIE TESTING OF POSTS	7
4.1 Test Matrix	7
4.2 Test Conditions	7
4.2.1 Bogie Vehicle	7
4.2.2 Bogie Tow and Guidance System	8
4.2.3 Post Installation Procedure	8
4.2.4 Data Acquisition Systems	8
4.2.4.1 Accelerometer	8
4.2.4.2 High-Speed Photography	11
4.2.4.3 Pressure Tape Switches	11
4.3 Test Results	11
5 COMPUTER SIMULATION	19
5.1 Background	19
5.2 Design Alternatives	19
5.3 BARRIER VII Results	20
6 W-BEAM GUARDRAIL ADJACENT TO A SLOPE DESIGN	24

7 TEST CONDITIONS	31
7.1 Test Facility	31
7.2 Vehicle Tow and Guidance System	31
7.3 Test Vehicle	31
7.4 Data Acquisition Systems	34
7.4.1 Accelerometers	34
7.4.2 Rate Transducer	36
7.4.3 High-Speed Photography	36
7.4.4 Pressure Tape Switches	37
8 CRASH TEST NO. 1	39
8.1 Test MOSW-1	39
8.2 Test Description	39
8.3 Barrier Damage	41
8.4 Vehicle Damage	42
8.5 Occupant Risk Values	42
8.6 Discussion	43
9 SUMMARY AND CONCLUSIONS	65
10 RECOMMENDATIONS	67
11 REFERENCES	68
12 APPENDICES	70
APPENDIX A - Force-Deflection Behavior of Bogie Tests	71
APPENDIX B - Typical BARRIER VII Input File	78
APPENDIX C - Accelerometer Data Analysis, Test MOSW-1	85
APPENDIX D - Roll, Pitch, and Yaw Data Analysis, Test MOSW-1	92

List of Figures

	Page
1. Post Installation Procedure	9
2. Typical Steel Post on Slope Break Point	10
3. Post Damage and Soil Failure, Bogie Test MSB-1	13
4. Post Damage and Soil Failure, Bogie Test MSB-2	14
5. Post Damage and Soil Failure, Bogie Test MSB-3	15
6. Post Damage and Soil Failure, Bogie Test MSB-4	16
7. Post Damage and Soil Failure, Bogie Test MSB-5	17
8. Post Damage and Soil Failure, Bogie Test MSB-6	18
9. W-beam Guardrail Adjacent to a 2:1 Foreslope System	26
10. W-beam Guardrail Adjacent to a 2:1 Foreslope	27
11. W-beam Guardrail Adjacent to a 2:1 Foreslope	28
12. W-beam Guardrail Adjacent to a 2:1 Foreslope	29
13. End Anchorage Systems	30
14. Test Vehicle, Test MOSW-1	32
15. Vehicle Dimensions, Test MOSW-1	33
16. Vehicle Target Locations, Test MOSW-1	35
17. Location of High-Speed Cameras, Test MOSW-1	38
18. Summary of Test Results and Sequential Photographs, Test MOSW-1	44
19. Additional Sequential Photographs, Test MOSW-1	45
20. Additional Sequential Photographs, Test MOSW-1	46
21. Documentary Photographs, Test MOSW-1	47
22. Documentary Photographs, Test MOSW-1	48
23. Documentary Photographs, Test MOSW-1	49
24. Impact Location, Test MOSW-1	50
25. Vehicle Final Position, Test MOSW-1	51
26. W-beam Guardrail System Damage, Test MOSW-1	52
27. W-beam Guardrail System Damage, Test MOSW-1	53
28. Post Nos. 15 and 16 Damage, Test MOSW-1	54
29. Post Nos. 17 and 18 Damage, Test MOSW-1	55
30. Post Nos. 19 and 20 Damage, Test MOSW-1	56
31. Post No. 19 Damage, Test MOSW-1	57
32. Post No. 20 Damage, Test MOSW-1	58
33. Post Nos. 21 and 22 Damage, Test MOSW-1	59
34. Post Nos. 23 and 24 Damage, Test MOSW-1	60
35. Post Nos. 25 and 26 Damage, Test MOSW-1	61
36. Permanent Set Deflections, Test MOSW-1	62
37. Vehicle Damage, Test MOSW-1	63
38. Vehicle Front-End Damage, Test MOSW-1	64
A-1. Graph of Force-Deflection Behavior, Test MSB-1	72
A-2. Graph of Force-Deflection Behavior, Test MSB-2	73

A-3. Graph of Force-Deflection Behavior, Test MSB-3	74
A-4. Graph of Force-Deflection Behavior, Test MSB-4	75
A-5. Graph of Force-Deflection Behavior, Test MSB-5	76
A-6. Graph of Force-Deflection Behavior, Test MSB-6	77
C-1. Graph of Longitudinal Deceleration, Test MOSW-1	86
C-2. Graph of Longitudinal Occupant Impact Velocity, Test MOSW-1	87
C-3. Graph of Longitudinal Occupant Displacement, Test MOSW-1	88
C-4. Graph of Lateral Deceleration, Test MOSW-1	89
C-5. Graph of Lateral Occupant Impact Velocity, Test MOSW-1	90
C-6. Graph of Lateral Occupant Displacement, Test MOSW-1	91
D-1. Graph of Roll Angular Displacements, Test MOSW-1	93
D-2. Graph of Pitch Angular Displacements, Test MOSW-1	94
D-3. Graph of Yaw Angular Displacements, Test MOSW-1	95

List of Tables

	Page
1. NCHRP Report No. 350 Evaluation Criteria for 2000P Pickup Truck Crash Test	6
2. Steel Post Bogie Impact Test Matrix	7
3. Steel Post Bogie Impact Test Results	12
4. Computer Simulation Results	22
5. Determination of Critical Impact Point	23
6. Summary of Safety Performance Evaluation Results - Slope W-beam Guardrail System . . .	66

1 INTRODUCTION

1.1 Problem Statement

When the Interstate Highway System was originally constructed across many Midwest states, W-beam guardrails were frequently installed at the slope break point adjacent to steep roadside slopes. This type of installation was generally used in restricted right-of-way situations where additional space for extending the fill slope could not be obtained. Continued economic development over the last three decades has not alleviated right-of-way restrictions at these sites. When 3R projects are implemented along these roadways, the safety performance of these guardrail installations comes into question.

Some of the standard strong-post W-beam guardrails installed adjacent to steep roadside slopes have been shown to perform satisfactorily, but with very large deflections. These crash testing efforts were evaluated according to the guidelines set forth in the National Cooperative Highway Research Program (NCHRP) Report No. 230, *Recommendation Procedures for the Safety Performance Evaluation of Highway Appurtenances* (1). However, these designs have never been tested according to the current guidelines. Therefore, it was necessary to evaluate the capacity of standard guardrails installed adjacent to steep roadside slopes, and if necessary, develop a new design that could meet the current evaluation criteria presented in NCHRP Report No. 350, *Recommended Procedures for the Safety Performance Evaluation of Highway Features* (2).

1.2 Objective

The objective of this research project was to evaluate the safety performance of standard W-beam guardrails installed at the slope break point of steep roadside slopes. The guardrail system was to be evaluated according to the Test Level 3 (TL-3) safety performance criteria set forth in the

NCHRP Report No. 350 (2). If necessary, a new guardrail system would then be designed and tested that could meet NCHRP Report No. 350 criteria when installed at the break point of a roadside foreslope as steep as 2:1.

1.3 Scope

The research objective was to be achieved by performing several tasks. First, a literature review was performed on previously crash tested guardrail systems with posts placed in or adjacent to sloped fill. Next, six dynamic bogie tests were performed on steel posts placed on the slope break point of a 2:1 foreslope in order to determine the post-soil response of various post and soil-embedment geometries. Following this phase, computer simulation modeling was undertaken to determine the optimum design for the guardrail system. After the final design was completed, the guardrail system was fabricated and constructed at the Midwest Roadside Safety Facility's (MwRSF's) outdoor test site. A full-scale vehicle crash test was then performed using a ¾-ton pickup truck, weighing approximately 2,000 kg, at a target impact speed and angle of 100.0 km/hr and 25 degrees, respectively. Finally, the test results were analyzed, evaluated, and documented. Conclusions and recommendations were then made that pertain to the safety performance of the guardrail system adjacent to a 2:1 foreslope.

2 LITERATURE REVIEW

Previous testing on W-beam guardrail systems adjacent to a slope was conducted by ENSCO, Inc. and was met with mixed results (3). The research study consisted of several static and dynamic pendulum tests on guardrail posts in soil as well as four full-scale vehicle crash tests on W-beam barriers. The crash testing of the W-beam guardrail systems adjacent to a slope was evaluated according to the criteria provided in NCHRP Report No. 230 (1).

The first impact consisted of a full-scale vehicle crash test on a standard G4(1S) guardrail system with the back-side flanges of 2.13-m long steel posts installed at the breakpoint of a 2:1 foreslope. The 2,044-kg passenger-size sedan, used in test no. 1717-1-88, impacted the rail and penetrated behind the system due to the failure of the upstream end anchor cable system.

Following the failure of test no. 1717-1-88, the guardrail system was modified by changing the upstream end anchor system to an eccentric loader BCT. The modified guardrail system was still configured with the back-side flanges of 2.13-m long steel posts installed at the breakpoint of a 2:1 foreslope. The 1,973-kg passenger-size sedan, used in test no. 1717-2-88, impacted the rail and began to redirect. Subsequently, the end anchor released slightly and allowed the rail height to drop, thus causing the vehicle to vault over the rail. The vehicle then rolled onto its side before coming to a rest.

A retest of test no. 1717-2-88 was then performed due to the upstream end anchor failure. The 1,970-kg passenger-size sedan, used in test no. 1717-3-88, impacted the rail and was redirected safely. However, it is noted that the vehicle's speed change was 11.2 m/s which was greater than the 6.7 m/s allowed by NCHRP Report No. 230.

The final full-scale vehicle crash test was performed on a standard G4(1S) guardrail system

with the back-side flanges of 1.83-m long steel posts installed at the breakpoint of a 2:1 foreslope. The 1,978-kg passenger-size sedan, used in test no. 1717-4-88, impacted the rail and was redirected. During the test, significant vehicle penetration into the rail system was observed. A high change in vehicle speed was also observed in this test similar to that found in test no. 1717-3-88. Finally, the vehicle showed no tendency to fall down the slope as it remained quite stable with little vehicle roll.

Following the completion of the study, ENSCO researchers concluded that a standard G4(1S) guardrail system with the back-side flanges of either 1,829-mm or 2,134-mm long steel posts installed at the breakpoint of a 2:1 slope will redirect a large sedan (NCHRP 230 – test designation 10). However, it was noted that the dynamic rail deflection for the 1,829-mm post length was approximately 1,219 mm. Therefore, the recommended post length for guardrails placed on the break point of a 2:1 slope was 2,134 mm.

3 TEST REQUIREMENTS AND EVALUATION CRITERIA

3.1 Test Requirements

Longitudinal barriers, such as W-beam guardrail systems for use on a 2:1 foreslope, must satisfy the requirements provided in NCHRP Report No. 350 to be accepted for use on new construction projects or as a replacement for existing systems when 3R projects are implemented where designs do not meet current safety standards. According to TL-3 of NCHRP Report No. 350, guardrail systems must be subjected to two full-scale vehicle crash tests: (1) a 2,000-kg pickup truck impacting at a speed of 100.0 km/hr and at an angle of 25 degrees; and (2) an 820-kg small car impacting at a speed of 100.0 km/hr and at an angle of 20 degrees. However, W-beam barriers struck by small cars have been shown to meet safety performance standards, with little lateral deflections (4-6), with no significant potential for occupant risk problems arising from vehicle pocketing or severe wheel snagging on the posts. Therefore, the 820-kg small car crash test was deemed unnecessary for this project.

3.2 Evaluation Criteria

Evaluation criteria for full-scale vehicle crash testing are based on three appraisal areas: (1) structural adequacy; (2) occupant risk; and (3) vehicle trajectory after collision. Criteria for structural adequacy are intended to evaluate the ability of the barrier to contain, redirect, or allow controlled vehicle penetration in a predictable manner. Occupant risk evaluates the degree of hazard to occupants in the impacting vehicle. Vehicle trajectory after collision is a measure of the potential for the post-impact trajectory of the vehicle to cause subsequent multi-vehicle accidents. It is also an indicator for the potential safety hazard for the occupants of the other vehicles or the occupants of the impacting vehicle when subjected to secondary collisions with other fixed objects. These three

evaluation criteria are defined in Table 1. The full-scale vehicle crash test was conducted and reported in accordance with the procedures provided in NCHRP Report No. 350.

Table 1. NCHRP Report No. 350 Evaluation Criteria for 2000P Pickup Truck Crash Test (2)

Structural Adequacy	A. Test article should contain and redirect the vehicle; the vehicle should not penetrate, underide, or override the installation although controlled lateral deflection of the test article is acceptable.
Occupant Risk	D. Detached elements, fragments or other debris from the test article should not penetrate or show potential for penetrating the occupant compartment, or present an undue hazard to other traffic, pedestrians, or personnel in a work zone. Deformations of, or intrusions into, the occupant compartment that could cause serious injuries should not be permitted.
	F. The vehicle should remain upright during and after collision although moderate roll, pitching, and yawing are acceptable.
Vehicle Trajectory	K. After collision it is preferable that the vehicle's trajectory not intrude into adjacent traffic lanes.
	L. The occupant impact velocity in the longitudinal direction should not exceed 12 m/sec and the occupant ridedown acceleration in the longitudinal direction should not exceed 20 G's.
	M. The exit angle from the test article preferably should be less than 60 percent of test impact angle, measured at time of vehicle loss of contact with test devise.

4 DEVELOPMENTAL TESTING – BOGIE TESTING OF POSTS

4.1 Test Matrix

Dynamic bogie testing was used to obtain the force-deflection behavior of various steel posts placed in soil and on the slope break point of a 2:1 foreslope. The steel guardrail posts were embedded in soil material conforming to AASHTO M147-65 Gradation “B” specifications (NCHRP Report No. 350 Strong Soil). The steel guardrail posts were impacted with a 972-kg bogie vehicle at the target speeds of 24.1 km/hr for the first five tests and 32.2 km/hr for the last test. All six of the steel posts were impacted 550 mm above the ground line and perpendicular to the front face of the posts. The test matrix for the six bogie tests is shown in Table 2.

Table 2. Steel Post Bogie Impact Test Matrix

Test No.	Post Type ASTM Designation	Embedment Depth (mm)	Target Speed (km/hr)
MSB-1	W152x17.9 by 2.44-m long	1,702	24.1
MSB-2	W152x17.9 by 2.44-m long	1,397	24.1
MSB-3	W152x13.4 by 2.13-m long	1,403	24.1
MSB-4	W152x13.4 by 2.13-m long	1,403	24.1
MSB-5	W152x13.4 by 2.13-m long	1,403	24.1
MSB-6	W152x17.9 by 2.95-m long	2,216	32.2

4.2 Test Conditions

4.2.1 Bogie Vehicle

A rigid frame bogie, constructed from Federal Highway Administration (FHWA)

specifications (Z), was used to impact the steel posts. The bogie was modified with a rigid cylinder impactor.

4.2.2 Bogie Tow and Guidance System

For each bogie test, a steel corrugated beam guardrail was used to guide the tire of the bogie. A pickup truck was used to push the bogie to the required impact velocity, at which point the pickup truck released, allowing the bogie to become a free projectile as it came off the guide track.

4.2.3 Post Installation Procedure

An area approximately 1727-mm wide and 1219-mm long with an approximate slope of 610 mm over 1219 mm was cut near the concrete apron. The posts were installed with the centerline of the post at 0.91 m from the edge of the concrete apron. The posts were installed by auguring 610-mm diameter holes at the slope break point. The 1.5-m deep holes were filled with soil material in 15-mm to 23-mm lifts and with optimum moisture (7% by dry weight). The material was tamped with an air tamper to a density of approximately 21.4 kN/m³. The typical post installation is shown in Figures 1 and 2.

4.2.4 Data Acquisition Systems

4.2.4.1 Accelerometer

A triaxial piezoresistive accelerometer system with a range of ± 200 G's was used to measure the acceleration in the longitudinal, lateral, and vertical directions at a sample rate of 3,200 Hz.. The environmental shock and vibrations sensor/recorder system, Model EDR-3, was developed by Instrumented Sensor Technology (IST) of Okemos, Michigan. The EDR-3 was configured with 256 Kb of RAM memory and a 1,120 Hz lowpass filter. Computer software, "DynaMax 1 (DM-1)" and "DADiSP" were used to digitize, analyze, and plot the accelerometer data.



Figure 1. Post Installation Procedure

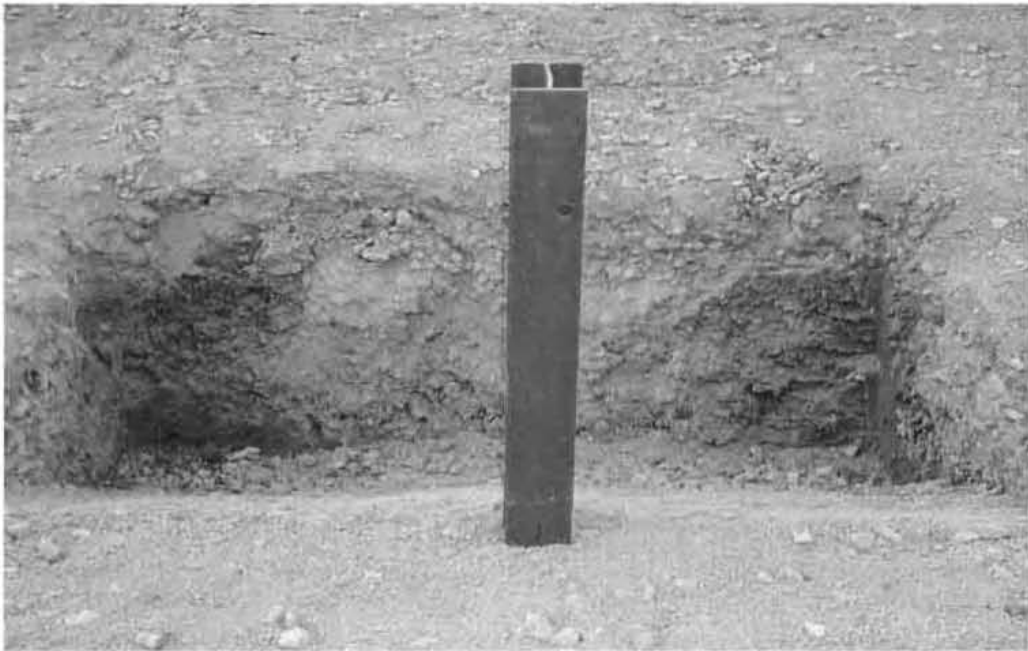


Figure 2. Typical Steel Post on Slope Break Point

4.2.4.2 High-Speed Photography

For bogie tests MSB-1 and MSB-2, a high-speed Red Lake E/cam video camera, with an operating speed of 500 frames/sec, was placed on the right side of the post and had a field of view perpendicular to the post. A SVHS video camera was also placed on the right side of the post and had a slightly angled view of the post and impact.

For bogie tests MSB-3 through MSB-6, a high-speed Red Lake E/cam video camera, with an operating speed of 500 frames/sec, was placed on the left side of the post and had a field of view perpendicular to the post. A Canon digital video camera was also placed on the left side of the post and had a slightly angled view of the post and impact.

4.2.4.3 Pressure Tape Switches

Three pressure-activated tape switches, spaced at 1-m intervals, were used to determine the speed of the bogie before impact. Each tape switch fired a strobe light which sent an electronic timing signal to the data acquisition system as the right-front tire of the test vehicle passed over it. Test bogie speeds were determined from electronic timing mark data recorded on "Test Point" software.

4.3 Test Results

Six bogie tests were performed and are summarized in Table 3. Force-deflection plots for each post test are shown graphically in Appendix A. Post damage and soil failure for each bogie test are shown in Figures 3 through 8. For all of the bogie impacts, it is noted that the primary mode of failure occurred in the soil rather than with post yielding.

Table 3. Steel Post Bogie Impact Test Results

Test No.	Speed (km/hr)	Peak Load (kN)	Deflection at Peak Load (mm)	Results
MSB-1	23.3	117.7	67.8	Small soil failure at front of post, post rotation
MSB-2	25.3	79.3	60.7	Large soil failure at front of post
MSB-3	23.2	64.6	63.5	457-mm radius soil failure at front of post
MSB-4	23.2	77.5	53.6	381-mm radius soil failure at front of post
MSB-5	21.7	41.3	72.9	305-mm radius soil failure at front of post
MSB-6	34.1	136.2	96.3	No soil failure at the front of the post, post slightly twisted during rotation, post bent 1.4 m from the top with maximum deflection of 121 mm



Figure 3. Post Damage and Soil Failure, Bogie Test MSB-1



Figure 4. Post Damage and Soil Failure, Bogie Test MSB-2

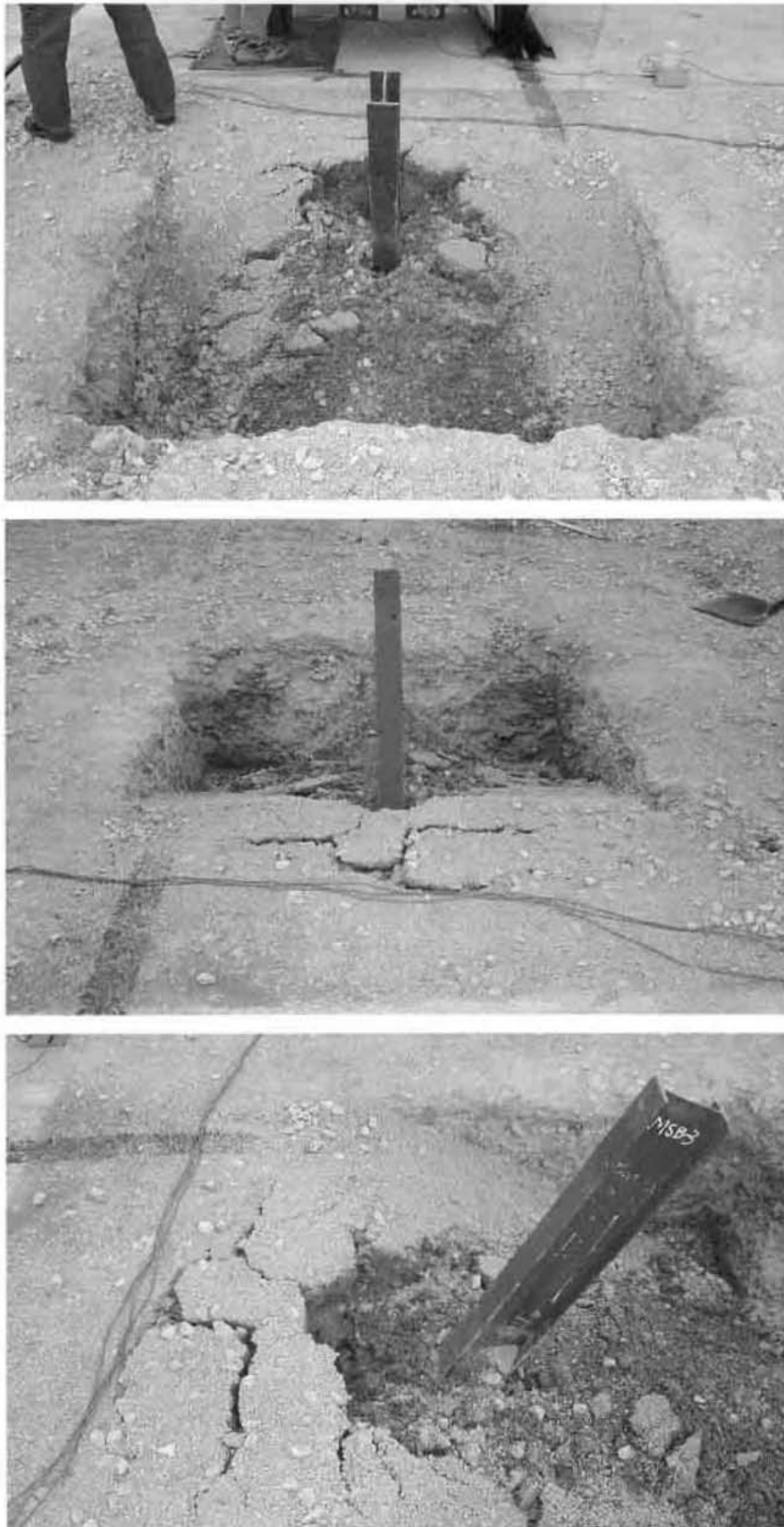


Figure 5. Post Damage and Soil Failure, Bogie Test MSB-3



Figure 6. Post Damage and Soil Failure, Bogie Test MSB-4

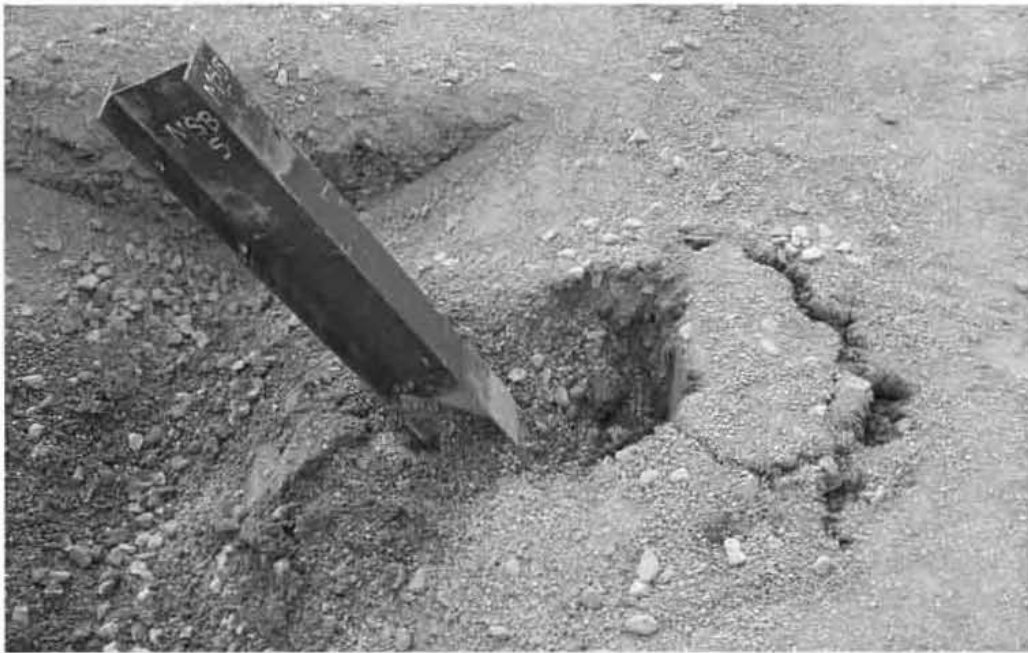


Figure 7. Post Damage and Soil Failure, Bogie Test MSB-5



Figure 8. Post Damage and Soil Failure, Bogie Test MSB-6

5 COMPUTER SIMULATION

5.1 Background

BARRIER VII computer simulation modeling (9) was incorporated in the development of the W-beam guardrail system for use on the slope break point of a 2:1 foreslope. First, a simulation was performed at the impact conditions of an actual crash test in order to calibrate selected input parameters for structural elements used in the model. The results from Texas Transportation Institute (TTI) crash test no. 405421-1, conducted on a strong-post, W-beam guardrail system, were used in the validation effort (10). Next, the data collected from the developmental bogie testing was used to model various design alternatives. During the development effort, several simulations were conducted modeling a 2000-kg pickup truck impacting at a speed of 100.0 km/hr and at an angle of 25 degrees. The simulations were conducted for each system to analyze the guardrail system and predict the dynamic deflection of the barrier. Finally, computer simulation was also used to determine the critical impact point (CIP) for the longitudinal barrier system. A typical computer simulation input data file is shown in Appendix B.

5.2 Design Alternatives

Computer simulation was performed on four basic design alternatives. All of the alternatives were configured for use on a 2:1 foreslope. They are as follows:

- (1) a W-beam barrier system with 2,134-mm long posts spaced 1,905 mm on center;
- (2) a W-beam barrier system with 2,438-mm long posts spaced 1,905 mm on center;
- (3) a W-beam barrier system with 2,134-mm long posts spaced 952.5 mm on center; and
- (4) a W-beam barrier system with 2,438-mm long posts spaced 952.5 mm on center.

5.3 BARRIER VII Results

The maximum dynamic deflection for strong-post, W-beam barrier systems typically range between 889 and 1,016 mm when impacted according to the TL-3 test conditions. For the development of the new guardrail system, MwRSF researchers deemed it prudent to maintain a maximum barrier deflection no more than that observed for barriers installed on level terrain or where a minimum width of 610 mm of fill placed behind the posts. This design limitation was believed to be necessary in order to reduce the potential for severe wheel snag on the exposed posts as the tire dropped down the sloped fill and to decrease the potential for climbing and vaulting over the W-beam rail.

The computer simulation results for the four design alternatives are shown in Table 4. The first two simulations shown in this table were for calibration and evaluation of the simulation model. For the first two design alternatives listed in Section 7.2, runs Slope7d and Slope8d, the simulation results indicate that excessive dynamic deflections would occur. As mentioned previously, excessive deflections could lead to wheel snag and/or vehicle vaulting. For the last two design alternatives listed in Section 7.2, the test results indicate that the longer post lengths, used in combination with a half-post spacing, would provide maximum dynamic deflections less than those observed for strong-post, W-beam guardrail systems tested on level ground. Subsequently, the design alternative with 2,134-mm long posts spaced 952.5 mm on center was chosen as the system to be evaluated by full-scale crash testing.

Computer simulation with BARRIER VII was also used to evaluate the CIP for the full-scale crash test. The CIP is normally selected to maximize the barrier deflection and the greatest potential for wheel snagging or vehicle pocketing on a splice post. Simulations used to select the CIP for the

guardrail adjacent to a slope are summarized in Table 5. For the 2,134-mm long posts spaced 952.5 mm on center design alternative, an impact at node 83 or 238-mm downstream of post no. 17 was estimated to represent the CIP for full-scale crash testing.

Table 4. Computer Simulation Results

Run No.	Impact Node	Impact Conditions		Maximum Dynamic Rail Deflection ¹ (mm)	Terrain Condition	Post Length (mm)	Post Spacing (mm)	Description Summary
		Speed (km/hr)	Angle (deg)					
Slope5d	52	101.5	25.5	993 @ Node 70	Level	1,829	1,905	Calibration to TTI test no. 405421-1.
Slope6d	83	100.0	25.0	889 @ Node 101	Level	1,829	1,905	Baseline simulation with 1,829-mm posts and standard spacing.
Slope7d	83	100.0	25.0	1,031 @ Node 103	Sloped	2,438	1,905	Sloped fill and 2,438-mm posts.
Slope8d	83	100.0	25.0	1,194 @ Node 101	Sloped	2,134	1,905	Sloped fill and 2,134-mm posts.
Slope6dHPS	83	100.0	25.0	566 @ Node 97	Level	1,829	952.5	Level fill and 1,829-mm posts with half-post spacing.
Slope7dHPS	83	100.0	25.0	668 @ Node 97	Sloped	2,438	952.5	Sloped fill and 2,438-mm posts with half-post spacing.
Slope8dHPS	83	100.0	25.0	757 @ Node 99	Sloped	2,134	952.5	Sloped fill and 2,134-mm posts with half-post spacing.

¹ - Lateral distance measured at the center height of the rail.

Table 5. Determination of Critical Impact Point

Run No.	Impact Node	Impact Conditions		Maximum Dynamic Rail Deflection ¹ (mm)	Terrain Condition	Post Length (mm)	Post Spacing (mm)	Description Summary
		Speed (km/hr)	Angle (deg)					
Slope8dHPS	83	100.0	25.0	757 @ Node 99	Sloped	2,134	952.5	Sloped fill and 2,134-mm posts with half-post spacing.
Slope8dHPSb	78	100.0	25.0	747 @ Node 94	Sloped	2,134	952.5	Sloped fill and 2,134-mm posts with half-post spacing.
Slope8dHPSc	79	100.0	25.0	752 @ Node 95	Sloped	2,134	952.5	Sloped fill and 2,134-mm posts with half-post spacing.
Slope8dHPSd	80	100.0	25.0	726 @ Node 96	Sloped	2,134	952.5	Sloped fill and 2,134-mm posts with half-post spacing.
Slope8dHPSe	81	100.0	25.0	737 @ Node 97	Sloped	2,134	952.5	Sloped fill and 2,134-mm posts with half-post spacing.
Slope8dHPSf	82	100.0	25.0	747 @ Node 98	Sloped	2,134	952.5	Sloped fill and 2,134-mm posts with half-post spacing.

¹ - Lateral distance measured at the center height of the rail.

6 W-BEAM GUARDRAIL ADJACENT TO A SLOPE DESIGN

The test installation consisted of 53.34 m of standard 2.66-mm thick (12-gauge) W-beam guardrail supported by steel posts, as shown in Figure 9. Anchorage systems similar to those used on tangent guardrail terminals were utilized on both the upstream and downstream ends of the guardrail system. Photographs of the test installation are shown in Figures 10 through 13.

The entire system was constructed with thirty-eight guardrail posts. Post nos. 3 through 11 and 31 through 36 were galvanized ASTM A36 steel W152x13.4 sections measuring 1,829-mm long. Post nos. 12 through 30 were also ASTM A36 steel W152x13.4 sections but measured 2,134-mm long. Post nos. 1, 2, 25, and 26 were timber posts measuring 140-mm wide x 190-mm deep x 1,080-mm long and were placed in steel foundation tubes. The timber posts and foundation tubes were part of anchor systems designed to replicate the capacity of a tangent guardrail terminal.

Post nos. 1 through 12 and 30 through 38 were spaced 1,905-mm on center. Post nos. 12 and 30 were spaced 952.5-mm on center, as shown in Figure 9. For post nos. 3 through 11 and 31 through 36, the soil embedment depth was 1,100 mm. For post nos. 12 through 30, the soil embedment depth was 1,404 mm. In addition, 150-mm wide x 200-mm deep x 360-mm long, routed wood spacer blockouts were used to block the rail away from post nos. 3 through 36, as shown in Figures 9, 11, and 12.

Seven standard 2.66-mm thick W-beam rails, each measuring 7,620-mm long, were placed between post nos. 1 and 38, as shown in Figure 9. The top mounting height of the W-beam rail was 706 mm. All lap-splice connections between the rail sections were configured to reduce vehicle snagging at the splice during the crash test.

A 2:1 foreslope pit was dug behind post nos. 12 through 30, as shown in Figures 11 and 12.

The maximum pit dimensions were 1830-mm wide and 915-mm deep. The length of the pit was 19.05 m, spanning from the midspan between post nos. 11 and 12 to the midspan between post nos. 30 and 31.

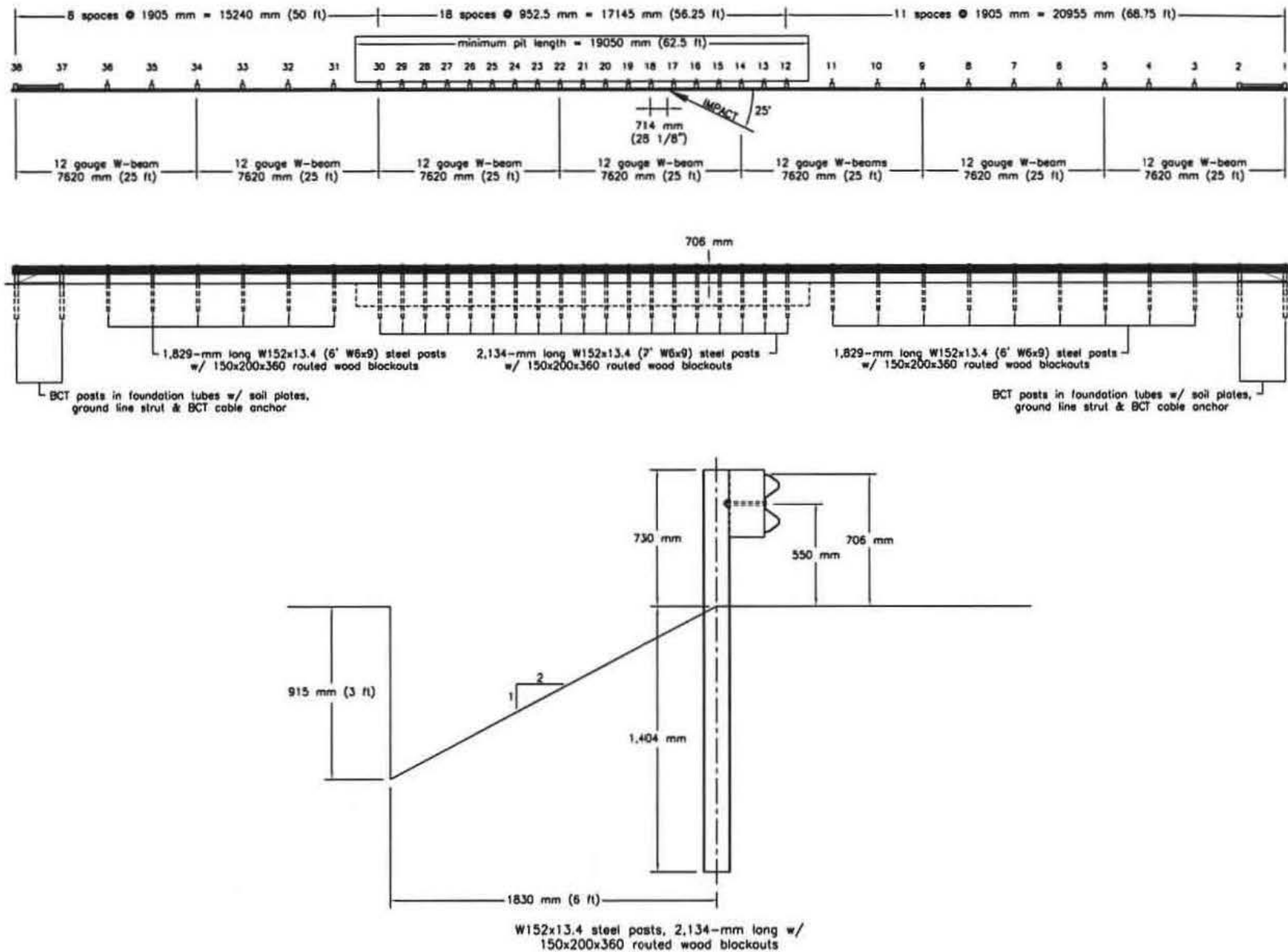


Figure 9. W-beam Guardrail Adjacent to a 2:1 Foreslope System



Figure 10. W-beam Guardrail Adjacent to a 2:1 Foreslope



Figure 11. W-beam Guardrail Adjacent to a 2:1 Foreslope



Figure 12. W-beam Guardrail Adjacent to a 2:1 Foreslope



Figure 13. End Anchorage Systems

7 TEST CONDITIONS

7.1 Test Facility

The testing facility is located at the Lincoln Air-Park on the northwest (NW) end of the Lincoln Municipal Airport and is approximately 8.0 km NW of the University of Nebraska-Lincoln.

7.2 Vehicle Tow and Guidance System

A reverse cable tow system with a 1:2 mechanical advantage was used to propel the test vehicle. The distance traveled and the speed of the tow vehicle were one-half that of the test vehicle. The test vehicle was released from the tow cable before impact with the guardrail. A digital speedometer in the tow vehicle was utilized to increase the accuracy of the test vehicle impact speed.

A vehicle guidance system developed by Hinch (8) was used to steer the test vehicle. A guide-flag, attached to the front-left wheel and the guide cable, was sheared off before impacting the guardrail. The 9.5-mm diameter guide cable was tensioned to approximately 13.3 kN, and supported by hinged stanchions in the lateral and vertical directions and spaced at 30.48 m initially and at 15.24 m toward the end of the guidance system. The hinged stanchions stood upright while holding up the guide cable, but as the vehicle was towed down the line, the guide-flag struck and knocked each stanchion to the ground. The vehicle guidance system was approximately 457.2-m long.

7.3 Test Vehicle

For test MOSW-1, a 1994 GMC 2500 ¾-ton pickup truck was used as the test vehicle. The test inertial and gross static weights were 2,024 kg. The test vehicle is shown in Figure 14, and vehicle dimensions are shown in Figure 15.

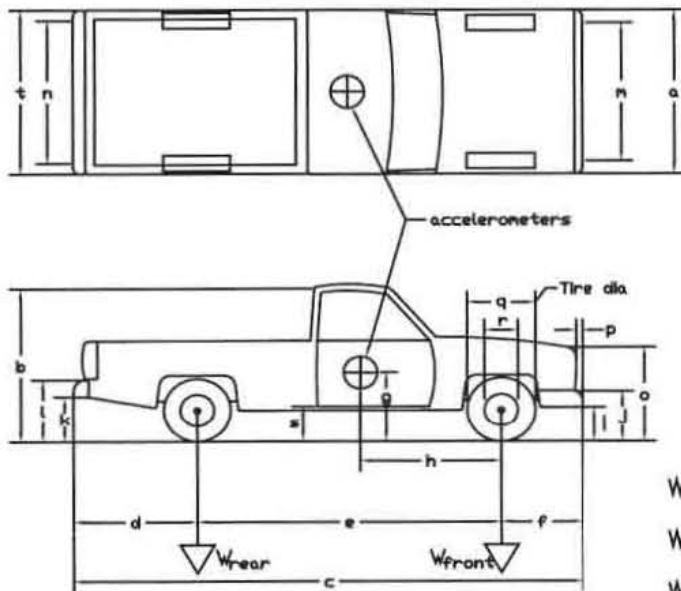
The longitudinal component of the center of gravity was determined using the measured axle weights. The location of the final center of gravity is shown in Figure 16.



Figure 14. Test Vehicle, Test MOSW-1

Date: 4/10/00 Test Number: MOSW-1 Model: 2500
 Make: GMC Vehicle I.D.#: 1GDC24K2RE550535
 Tire Size: 245/75 R16 Year: 1994 Odometer: 199887

*(All Measurements Refer to Impacting Side)



Vehicle Geometry - mm

a 1930 b 1835
 c 5563 d 1302
 e 3327 f 908
 g 737 h 1415
 i 432 j 635
 k 610 l 800
 m 1594 n 1626
 o 1003 p 102
 q 749 r 445
 s 483 t 1848

Wheel Center Height Front 362
 Wheel Center Height Rear 370
 Wheel Well Clearance (FR) 889
 Wheel Well Clearance (RR) 959

Engine Type 8 CYL. GAS

Engine Size 5.7 L 350 CID

Transmission Type:

(Automatic) or Manual

FWD or (RWD) or 4WD

Weights - kg	Curb	Test Inertial	Gross Static
W_{front}	<u>1193</u>	<u>1164</u>	<u>1164</u>
W_{rear}	<u>892</u>	<u>860</u>	<u>860</u>
W_{total}	<u>2085</u>	<u>2024</u>	<u>2024</u>

Note any damage prior to test: BOX DAMAGE BEHIND REAR TIRES
DENT FRONT BUMPER
DRIVER DOOR AND FENDER JOINT DAMAGE

Figure 15. Vehicle Dimensions, Test MOSW-1

Square, black and white-checked targets were placed on the vehicle to aid in the analysis of the high-speed film, as shown in Figure 16. One target was placed on the center of gravity on the driver's side door, the passenger's side door, and on the roof of the vehicle. The remaining targets were located for reference so that they could be viewed from the high-speed cameras for film analysis.

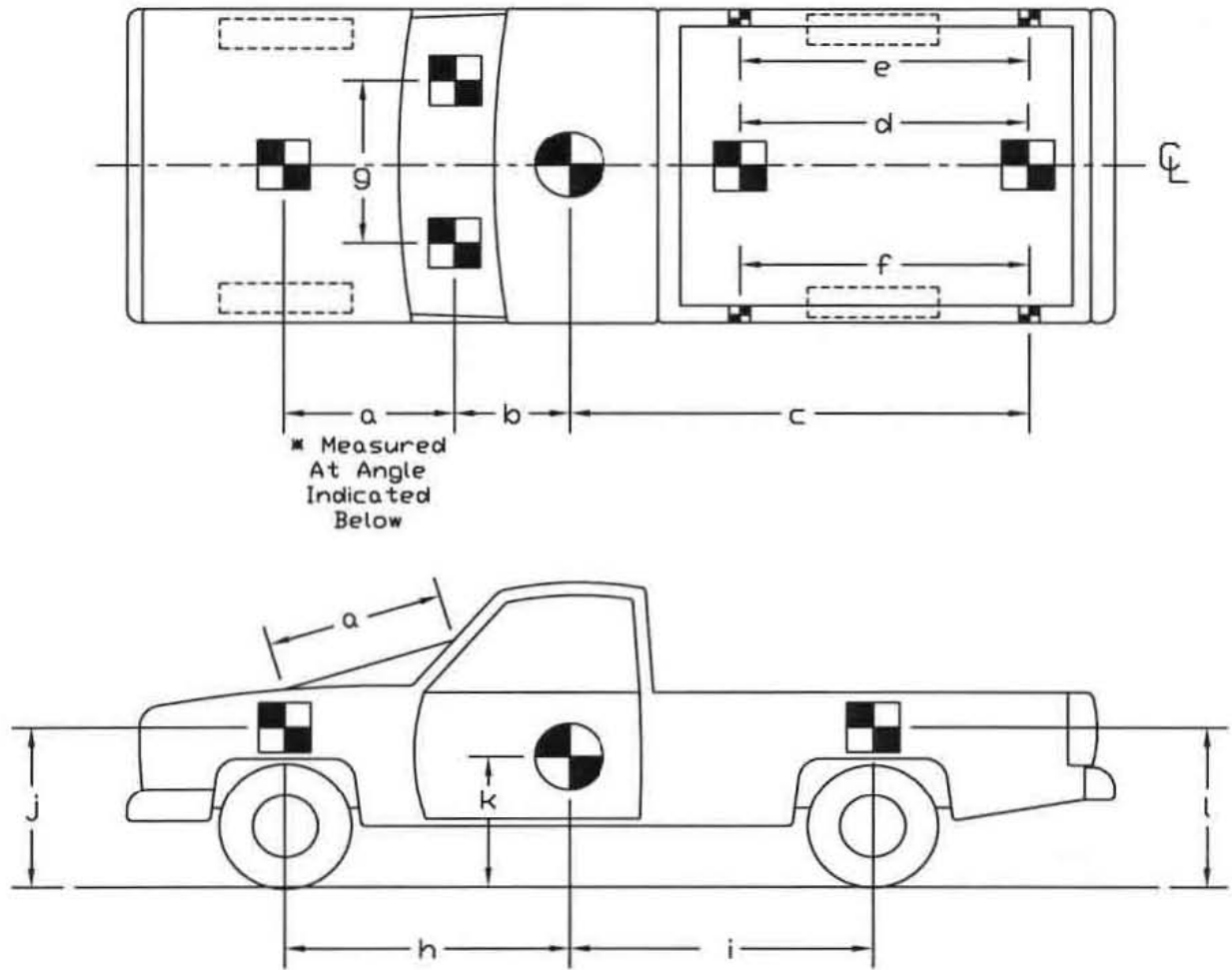
The front wheels of the test vehicle were aligned for camber, caster, and toe-in values of zero so that the vehicle would track properly along the guide cable. Two 5B flash bulbs were mounted on both the hood and roof of the vehicle to pinpoint the time of impact with the guardrail on the high-speed film. The flash bulbs were fired by a pressure tape switch mounted on the front face of the bumper. A remote controlled brake system was installed in the test vehicle so the vehicle could be brought safely to a stop after the test.

7.4 Data Acquisition Systems

7.4.1 Accelerometers

One triaxial piezoresistive accelerometer system with a range of ± 200 G's was used to measure the acceleration in the longitudinal, lateral, and vertical directions at a sample rate of 10,000 Hz. The environmental shock and vibration sensor/recorder system, Model EDR-4M6, was developed by Instrumented Sensor Technology (IST) of Okemos, Michigan and includes three differential channels as well as three single-ended channels. The EDR-4 was configured with 6 Mb of RAM memory and a 1,500 Hz lowpass filter. Computer software, "DynaMax 1 (DM-1)" and "DADiSP" were used to digitize, analyze, and plot the accelerometer data.

A backup triaxial piezoresistive accelerometer system with a range of ± 200 G's was also used to measure the acceleration in the longitudinal, lateral, and vertical directions at a sample rate of



TEST #: MOSW-1

TARGET GEOMETRY (mm)

a	959	d	1816	g	1048	j	994
b	730	e	2153	h	1415	k	737
c	2731	f	2153	i	1913	l	1060

Figure 16. Vehicle Target Locations, Test MOSW-1

3,200 Hz. The environmental shock and vibration sensor/recorder system, Model EDR-3, was developed by Instrumented Sensor Technology (IST) of Okemos, Michigan. The EDR-3 was configured with 256 Kb of RAM memory and a 1,120 Hz lowpass filter. Computer software, "DynaMax 1 (DM-1)" and "DADiSP" were used to digitize, analyze, and plot the accelerometer data.

7.4.2 Rate Transducer

A Humphrey 3-axis rate transducer with a range of 360 deg/sec in each of the three directions (pitch, roll, and yaw) was used to measure the rates of motion of the test vehicle. The rate transducer was rigidly attached to the vehicle near the center of gravity of the test vehicle. Rate transducer signals, excited by a 28 volt DC power source, were received through the three single-ended channels located externally on the EDR-4M6 and stored in the internal memory. The raw data measurements were then downloaded for analysis and plotted. Computer software, "DynaMax 1 (DM-1)" and "DADiSP" were used to digitize, analyze, and plot the rate transducer data.

7.4.3 High-Speed Photography

For test MOSW-1, five high-speed 16-mm Red Lake Locam cameras, with operating speeds of approximately 500 frames/sec, were used to film the crash test. One high-speed Red Lake E/cam video camera, with an operating speed of 500 frames/sec, was used to film the crash test. A Locam, with a wide-angle 12.5-mm lens, was placed above the test installation to provide a field of view perpendicular to the ground. A Locam with a 76 mm lens, a SVHS video camera, and a 35-mm still camera were placed downstream from the impact point and had a field of view parallel to the barrier. A Locam, with a 16 to 64-mm zoom lens, and a SVHS video camera were placed on the traffic side of the barrier and had a field of view perpendicular to the barrier. A Locam and a SVHS video camera were placed upstream and behind the barrier. Another Locam and a Canon digital video

camera were placed downstream and behind the barrier. A Red Lake E/cam high-speed video camera was placed downstream and behind the barrier. A schematic of all eleven camera locations for test MOSW-1 is shown in Figure 17. The film was analyzed using the Vanguard Motion Analyzer. Actual camera speed and camera divergence factors were considered in the analysis of the high-speed film.

7.4.4 Pressure Tape Switches

For test MOSW-1, five pressure-activated tape switches, spaced at 2-m intervals, were used to determine the speed of the vehicle before impact. Each tape switch fired a strobe light which sent an electronic timing signal to the data acquisition system as the left-front tire of the test vehicle passed over it. Test vehicle speed was determined from electronic timing mark data recorded on "Test Point" software. Strobe lights and high-speed film analysis are used only as a backup in the event that vehicle speed cannot be determined from the electronic data.

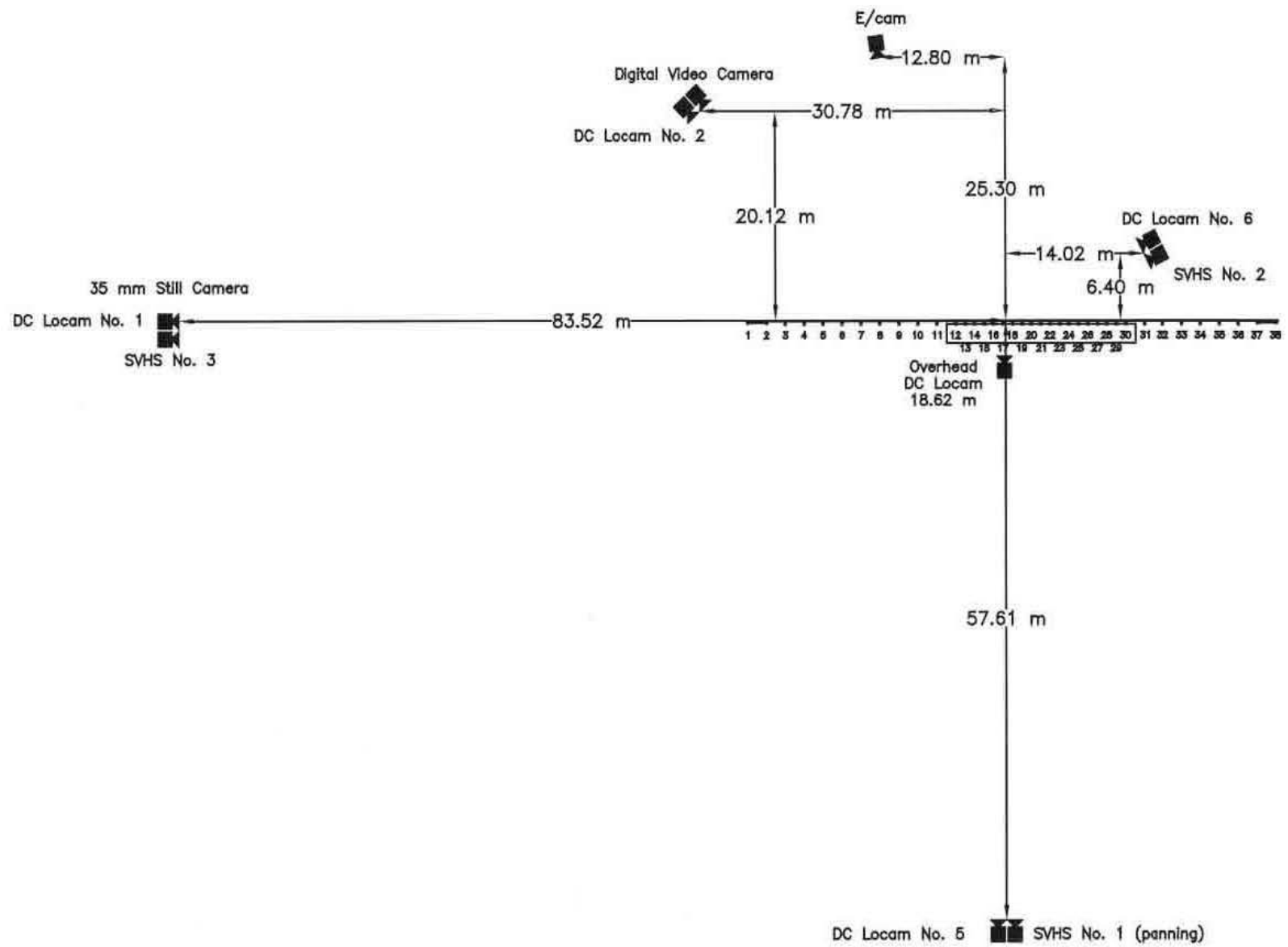


Figure 17. Location of High-Speed Cameras, Test MOSW-1

8 CRASH TEST NO. 1

8.1 Test MOSW-1

The 2,024-kg pickup truck impacted the new W-beam guardrail system at a speed of 100.7 km/hr and at an angle of 28.5 degrees. A summary of the test results and the sequential photographs are shown in Figure 18. Additional sequential photographs are shown in Figures 19 and 20. Documentary photographs of the crash test are shown in Figures 21 through 23.

8.2 Test Description

Initial impact occurred between post nos. 17 and 18 or 238-mm downstream from the center of post no. 17, as shown in Figure 24. At 0.031 sec after impact, the right-front corner of the vehicle was at post no. 18 which was deflecting backward. At this same time, the right corner of the bumper and the right-front fender were crushing inward as the hood protruded over the rail. At this same time, the rail was flattening. At 0.038 sec, post nos. 17 and 18 were deflected significantly backward. At 0.047 sec, post no. 19 deflected backward quickly. At 0.069 sec, the right-front parking light disengaged from the vehicle. At 0.074 sec, the right-front corner of the vehicle was at post no. 19. At this same time, post no. 20 encountered significant deflection as the guardrail in front of the vehicle began to push backward and lay down. At 0.100 sec, the wooden blockout at post no. 19 began to split. At 0.117 sec, the right-front corner of the vehicle was at post no. 20. At 0.124 sec, the interaction between the right-front corner of the vehicle and the rail caused the right-front corner to pitch down toward the ground. At this same time, the left-rear corner of the vehicle began to rise into the air. At 0.138 sec, the wood blockout at post no. 18 detached from the system. At 0.155 sec, the left-front tire became airborne. At 0.141 sec, a large piece of the wooden blockout at post no. 19 detached from the system and became airborne. At 0.177 sec, post no. 21 deflected

backward. At this same time, the right-front fender and right side of the bumper crushed inward as the right-front corner of the engine hood and upper edge of the right-front fender became separated. At 0.200 sec, the right-front corner of the vehicle was at post no. 21, and post no. 22 began to deflect significantly. At this same time, the wooden blockout at post no. 20 began to fracture as the vehicle began to redirect. At 0.206 sec, the left-rear tire became airborne as the vehicle encountered significant counter-clockwise (CCW) roll toward the rail. At 0.247 sec, the right-front corner of the vehicle was at post no. 22. At 0.286 sec, the right-front corner of the vehicle was at post no. 23 as the vehicle continued to roll CCW into the rail. At 0.271 sec, the right rear of the vehicle contacted the rail. At 0.315 sec, the left-front tire was at its highest point in the air, and the right rear of the vehicle rose into the air, indicating rail contact. At 0.321 sec, the truck was parallel with the rail and had a velocity of 55.72 km/hr. At 0.333 sec, the right-front corner of the vehicle was at post no. 24. At 0.395 sec, the right-front corner of the vehicle was at post no. 25, and the vehicle encountered significant roll toward the rail. At 0.412 sec, the right-front corner of the vehicle was no longer in contact with the rail. At 0.546 sec, the right-rear tire was the only vehicle component still in contact with the rail. At this same time, the right-front tire was the only tire in contact with the ground. At 0.608 sec after impact, the vehicle exited the guardrail at an angle of 25.8 degrees and a speed of 50.30 km/hr. At 0.660 sec, the rear-end of the vehicle continued to ascend into the air. At 0.872 sec, the rear of the vehicle rolled away from the rail. At 1.058 sec, vehicle roll ceased, and the vehicle reached its maximum pitch angle. At 1.596 sec, the right-rear tire contacted the ground, and the vehicle began to yaw clockwise (CW). Shortly after this time, the rear of the vehicle bounced up off the ground. At 2.289 sec, the rear of the vehicle was back on the ground. The vehicle came to rest 27.84-m downstream from impact and 2.13-m laterally away from the traffic-side face of the rail,

as shown in Figures 18 and 25.

8.3 Barrier Damage

Damage to the barrier was moderate, as shown in Figures 26 through 35. Barrier damage consisted mostly of deformed W-beam, contact marks on a guardrail section, and deformed guardrail posts. The W-beam damage consisted of moderate deformation and flattening of the lower portion of the impacted section between post nos. 17 and 25. Contact marks were found on the guardrail between post nos. 17 and 25. The W-beam rail was pulled off of post nos. 18 through 21.

Steel post nos. 3 through 11 twisted in the CW direction when viewed from the traffic-side face of the rail. Steel post nos. 12 through 16 also twisted CW and were slightly rotated backward. Steel post nos. 17 and 18 twisted and rotated backward with major soil failure visible at the ground level. The front flanges on steel post nos. 19 and 20 encountered moderate plastic deformations due to the wheel contact with the posts. Post yielding damage was also found on post nos. 19 and 20, as shown in Figures 31 and 32. Steel post nos. 19 through 23 twisted CW, rotated, and were bent toward the ground. Steel post nos. 24 through 26 rotated backward. No significant post damage occurred to post nos. 27 through 36. Both the upstream and downstream anchorage systems were slightly moved longitudinally, but the posts were not damaged.

The wooden blockout at post no. 19 split and rotated CCW around to the upstream side of the post. The blockout at post no. 20 disengaged from the system. The wooden blockout at post nos. 21 and 23 rotated CW when viewed from the front face of the post. The wooden blockout at post no. 22 split in half, while the blockouts at post nos. 3 through 18 and 25 through 36 remained undamaged.

The permanent set of the guardrail and posts is shown in Figures 28 through 35. The cable

anchor ends encountered slight permanent set deformations, as shown in Figure 36. The maximum lateral permanent set rail and post deflections were approximately 587 mm at the centerline of post no. 22 and 864 mm at post no. 21, respectively, as measured in the field. The maximum lateral dynamic rail and post deflections were 821 mm at the centerline of post no. 20 and 821 mm at post no. 20, respectively, as determined from the high-speed film analysis.

8.4 Vehicle Damage

Exterior vehicle damage was minimal, as shown in Figures 37 and 38. Interior occupant compartment deformations were determined to be negligible. The right-front quarter panel was crushed inward and downward, and the right side of the front bumper was also bent back toward the engine compartment. The right-front wheel assembly was deformed slightly, including contact marks and slight deformations on the rim and disengagement of the tie-rod. The right-front tire was also deflated. Small contact marks were found on the lower-right side of the front fender and right-side door frame. The grill was only broken and deformed around the right-side headlight. No other damage to the vehicle was observed.

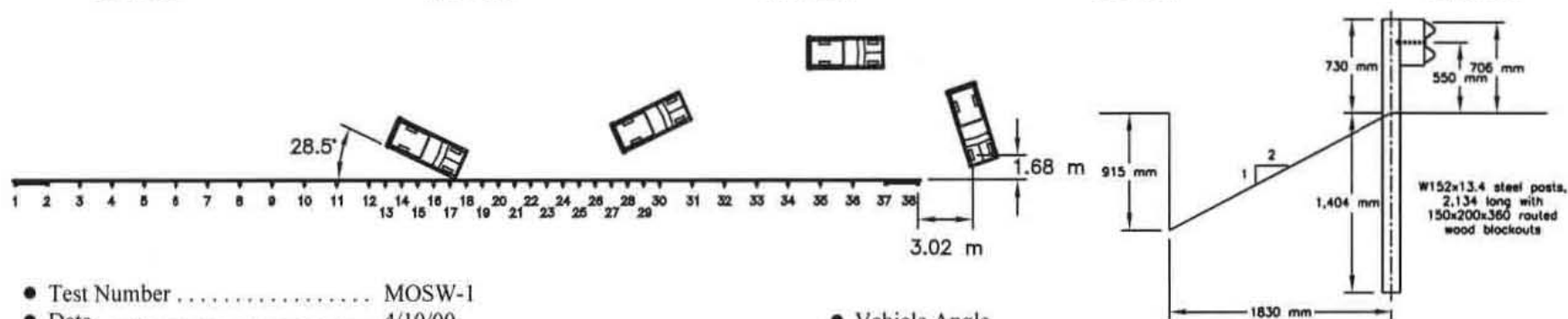
8.5 Occupant Risk Values

The longitudinal and lateral occupant impact velocities were determined to be 7.09 m/sec and 4.74 m/sec, respectively. The maximum 0.010-sec average occupant ridedown decelerations in the longitudinal and lateral directions were 7.80 g's and 9.54 g's, respectively. It is noted that the occupant impact velocities (OIV's) and occupant ridedown decelerations (ORD's) were within the suggested limits provided in NCHRP Report No. 350. The results of the occupant risk, determined from the accelerometer data, are summarized in Figure 18. Results are shown graphically in Appendix C. Due to technical difficulties, the rate transducer did not collect the roll, pitch, and yaw

data. However, roll, pitch, and yaw data were collected from film analysis and are shown graphically in Appendix D.

8.6 Discussion

The analysis of the test results for test MOSW-1 showed that the W-beam guardrail at the break point of a 2:1 slope adequately contained and redirected the vehicle with controlled lateral displacements of the guardrail. Detached elements and debris from the test article did not penetrate or show potential for penetrating the occupant compartment. Deformations of, or intrusion into, the occupant compartment that could have caused serious occupant injury did not occur. The vehicle remained upright during and after collision. Vehicle roll, pitch, and yaw angular displacements were noted, but they were deemed acceptable and did not adversely influence occupant risk safety criteria nor cause rollover. After collision, the vehicle's trajectory intruded slightly into adjacent traffic lanes but was determined to be acceptable. In addition, the vehicle's exit angle was less than 60 percent of the impact angle. Therefore, test MOSW-1 conducted on the W-beam guardrail system for use a 2:1 foreslope was determined to be acceptable according to the TL-3 criteria found in the NCHRP Report No. 350.



- Test Number MOSW-1
- Date 4/10/00
- Appurtenance W-beam guardrail system for use on a 2:1 foreslope
- Total Length 53.34 m
- Steel W-beam
 - Thickness 2.66 mm
 - Top Mounting Height 706 mm
- Steel Posts
 - Post Nos. 3 - 11, 31 - 36 W152x13.4 by 1,829-mm long
 - Post Nos. 12 - 30 W152x13.4 by 2,134-mm long
- Wood Posts
 - Post Nos. 1 - 2, 37 - 38 (BCT) 140 mm x 190 mm by 1,080-mm long
- Wood Spacer Blocks
 - Post Nos. 3 - 36 150 mm x 200 mm by 360-mm long
- Soil Type Grading B - AASHTO M 147-65 (1990)
- Vehicle Model 1994 GMC 2500 2WD
 - Curb 2,085 kg
 - Test Inertial 2,024 kg
 - Gross Static 2,024 kg
- Vehicle Speed
 - Impact 100.7 km/hr
 - Exit 50.30 km/hr

- Vehicle Angle
 - Impact 28.5 degrees
 - Exit 25.8 degrees
- Vehicle Snagging Minor wheel snagging on post nos. 18 through 20
- Vehicle Pocketing None
- Vehicle Stability Satisfactory
- Occupant Ridedown Deceleration (10 msec avg.)
 - Longitudinal 7.80 < 20 G's
 - Lateral (not required) 9.54
- Occupant Impact Velocity
 - Longitudinal 7.09 < 12 m/s
 - Lateral (not required) 4.74
- Vehicle Damage Minimal
 - TAD¹¹ 1-RFQ-3
 - SAE¹² 1-RFEE3
- Vehicle Stopping Distance 27.84 m downstream
2.13 m traffic-side face
- Barrier Damage Moderate
- Maximum Rail Deflections
 - Permanent Set 587 mm
 - Dynamic 821 mm

Figure 18. Summary of Test Results and Sequential Photographs, Test MOSW-1



0.000 sec



0.124 sec



0.177 sec



0.268 sec



0.412 sec



0.546 sec



0.000 sec



0.109 sec



0.172 sec



0.257 sec



0.342 sec



0.441 sec

Figure 19. Additional Sequential Photographs, Test MOSW-1



0.000 sec



0.069 sec



0.100 sec



0.141 sec



0.187 sec



0.271 sec



0.000 sec



0.148 sec



0.194 sec



0.318 sec



0.784 sec

Figure 20. Additional Sequential Photographs, Test MOSW-1



Figure 21. Documentary Photographs, Test MOSW-1



Figure 22. Documentary Photographs, Test MOSW-1



Figure 23. Documentary Photographs, Test MOSW-1



Figure 24. Impact Location, Test MOSW-1



Figure 25. Vehicle Final Position, Test MOSW-1



Figure 26. W-beam Guardrail System Damage, Test MOSW-1

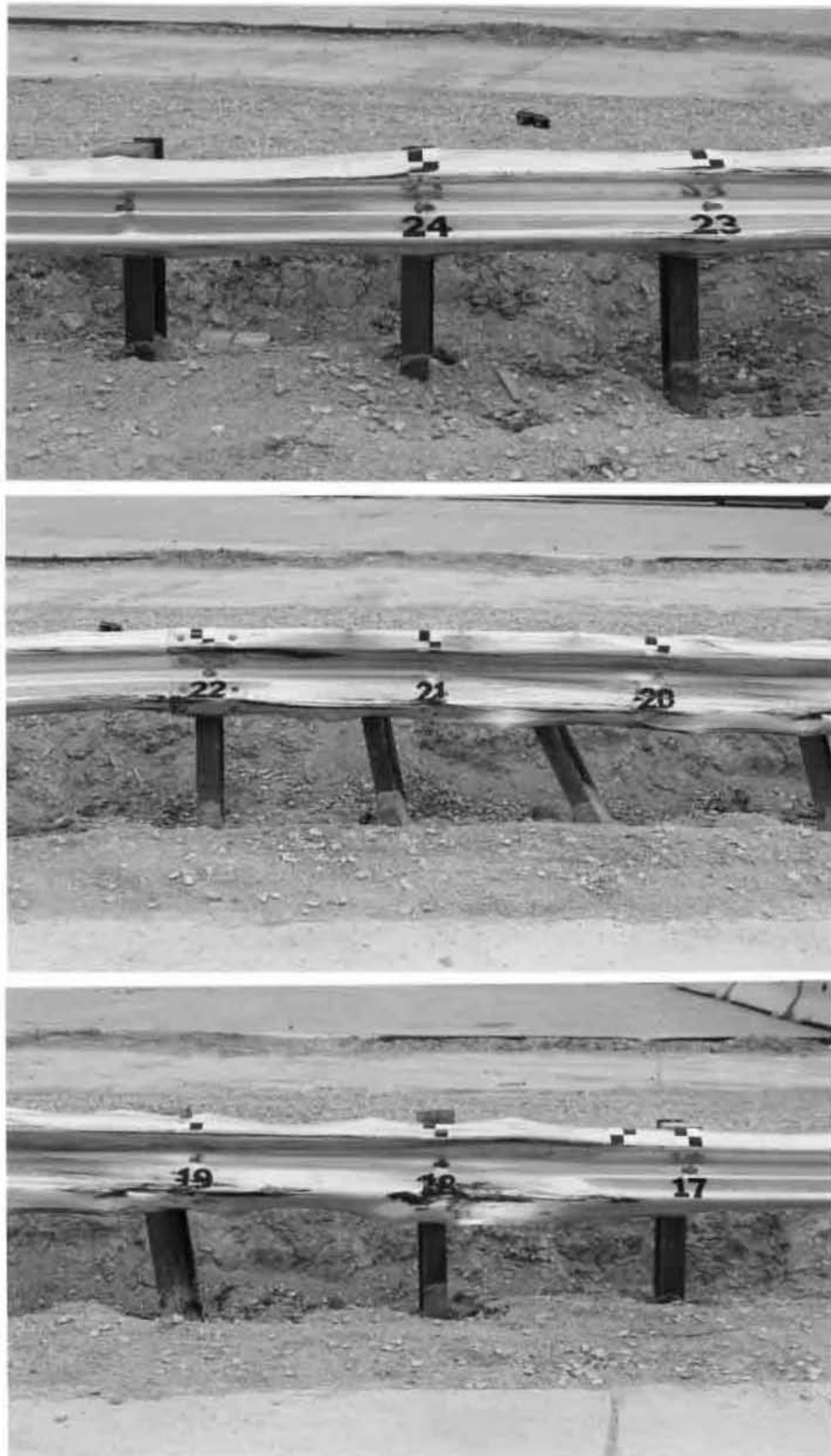


Figure 27. W-beam Guardrail System Damage, Test MOSW-1



Figure 28. Post Nos. 15 and 16 Damage, Test MOSW-1



Figure 29. Post Nos. 17 and 18 Damage, Test MOSW-1



Figure 30. Post Nos. 19 and 20 Damage, Test MOSW-1



Figure 31. Post No. 19 Damage, Test MOSW-1



Figure 32. Post No. 20 Damage, Test MOSW-1



Figure 33. Post Nos. 21 and 22 Damage, Test MOSW-1



Figure 34. Post Nos. 23 and 24 Damage, Test MOSW-1



Figure 35. Post Nos. 25 and 26 Damage, Test MOSW-1



Figure 36. Permanent Set Deflections, Test MOSW-1



Figure 37. Vehicle Damage, Test MOSW-1



Figure 38. Vehicle Front-End Damage, Test MOSW-1

9 SUMMARY AND CONCLUSIONS

A W-beam guardrail, designed for use on a 2:1 foreslope, was successfully developed and subjected to full-scale vehicle crash testing. The new guardrail system was configured with W-beam guardrail and supported by 2,134-mm long steel posts spaced on 952.5-mm centers. A full-scale vehicle crash test was performed with a ¾-ton pickup truck on the guardrail system and was determined to be acceptable according to the TL-3 safety performance criteria presented in NCHRP Report No. 350. A summary of the safety performance evaluation is provided in Table 6.

Table 6. Summary of Safety Performance Evaluation Results - Slope W-beam Guardrail System

Evaluation Factors	Evaluation Criteria	Test MOSW-1
Structural Adequacy	A. Test article should contain and redirect the vehicle; the vehicle should not penetrate, underide, or override the installation although controlled lateral deflection of the test article is acceptable.	S
Occupant Risk	D. Detached elements, fragments or other debris from the test article should not penetrate or show potential for penetrating the occupant compartment, or present an undue hazard to other traffic, pedestrians, or personnel in a work zone. Deformations of, or intrusions into, the occupant compartment that could cause serious injuries should not be permitted.	S
	F. The vehicle should remain upright during and after collision although moderate roll, pitching and yawing are acceptable.	S
Vehicle Trajectory	K. After collision it is preferable that the vehicle's trajectory not intrude into adjacent traffic lanes.	S
	L. The occupant impact velocity in the longitudinal direction should not exceed 12 m/sec and the occupant ridedown acceleration in the longitudinal direction should not exceed 20 G's.	S
	M. The exit angle from the test article preferably should be less than 60 percent of test impact angle, measured at time of vehicle loss of contact with test device.	S

S - (Satisfactory)
 M - (Marginal)
 U - (Unsatisfactory)
 NA - Not Available

10 RECOMMENDATIONS

A W-beam guardrail system designed for use on a 2:1 foreslope, as described in this report, was developed and successfully crash tested according to the criteria found in NCHRP Report No. 350. The results of this test indicate that this design is a suitable design for use on Federal-aid highways. It is suggested that the research described herein could be further developed using the data collected from testing to modify future designs. However, any design modifications made to the W-beam guardrail system on a foreslope may require verification through the use of full-scale vehicle crash testing.

Finally, it is recommended that future research be dedicated for the further optimization of guardrail designs for use on roadsides with sloped fill. It is noted that since test no. MOSW-1 was successful, it is unclear as to the magnitude of the factor of safety provided by the design described herein. Thus, it may be possible to obtain acceptable safety performance from a guardrail design which incorporates longer posts, a wider post spacing, or combinations thereof.

11 REFERENCES

1. Michie, J.D., *Recommended Procedures for the Safety Performance Evaluation of Highway Appurtenances*, National Cooperative Highway Research Program (NCHRP) Report No. 230, Transportation Research Board, Washington, D.C., March 1981.
2. Ross, H.E., Sicking, D.L., Zimmer, R.A. and Michie, J.D., *Recommended Procedures for the Safety Performance Evaluation of Highway Features*, National Cooperative Research Program (NCHRP) Report No. 350, Transportation Research Board, Washington, D.C., 1993.
3. Stout, D., Hinch, J., and Yang, T-L., *Force-Deflection Characteristics of Guardrail Posts*, Report No. FHWA-RD-88-195, Submitted to the Safety Design Division, Federal Highway Administration, Performed by ENSCO, Inc., August 31, 1988.
4. Buth, C.E., Campise, W.L., Griffin, III, L.I., Love, M.L., and Sicking, D.L., *Performance Limits of Longitudinal Barrier Systems - Volume I - Summary Report*, Report No. FHWA/RD-86/153, Submitted to the Office of Safety and Traffic Operations, Federal Highway Administration, Performed by Texas Transportation Institute, May 1986.
5. Ivey, D.L., Robertson, R., and Buth, C.E., *Test and Evaluation of W-Beam and Thrie-Beam Guardrails*, Report No. FHWA/RD-82/071, Submitted to the Office of Research, Federal Highway Administration, Performed by Texas Transportation Institute, March 1986.
6. Ross, H.E., Jr., Perera, H.S., Sicking, D.L., and Bligh, R.P., *Roadside Safety Design for Small Vehicles*, National Cooperative Highway Research Program (NCHRP) Report No. 318, Transportation Research Board, Washington, D.C., May 1989.
7. Hargrave, M.W., and Hansen, A.G., *Federal Outdoor Impact Laboratory - A New Facility for Evaluating Roadside Safety Hardware*, Transportation Research Record 1198, Transportation Research Board, National Research Council, Washington, D.C., 1988, pp. 90-96.
8. Hinch, J., Yang, T-L, and Owings, R., *Guidance Systems for Vehicle Testing*, ENSCO, Inc., Springfield, VA 1986.
9. Powell, G.H., *BARRIER VII: A Computer Program For Evaluation of Automobile Barrier Systems*, Prepared for: Federal Highway Administration, Report No. FHWA RD-73-51, April 1973.
10. Buth, C.E., Menges, W.L., Ivey, D.L., and Williams, W.F., *W-Beam Guardrail*, Paper accepted for publication at the 78th Annual Meeting of the Transportation Research Board, Washington, D.C., Paper No. 990871, January, 1999.

11. *Vehicle Damage Scale for Traffic Investigators*, Second Edition, Technical Bulletin No. 1, Traffic Accident Data (TAD) Project, National Safety Council, Chicago, Illinois, 1971.
12. *Collision Deformation Classification - Recommended Practice J224 March 1980*, Handbook Volume 4, Society of Automotive Engineers (SAE), Warrendale, Pennsylvania, 1985.

12 APPENDICES

APPENDIX A

Force-Deflection Behavior of Bogie Tests

Figure A-1. Graph of Force-Deflection Behavior, Test MSB-1

Figure A-2. Graph of Force-Deflection Behavior, Test MSB-2

Figure A-3. Graph of Force-Deflection Behavior, Test MSB-3

Figure A-4. Graph of Force-Deflection Behavior, Test MSB-4

Figure A-5. Graph of Force-Deflection Behavior, Test MSB-5

Figure A-6. Graph of Force-Deflection Behavior, Test MSB-6

W14: Force vs. Displacement - Test MSB-1

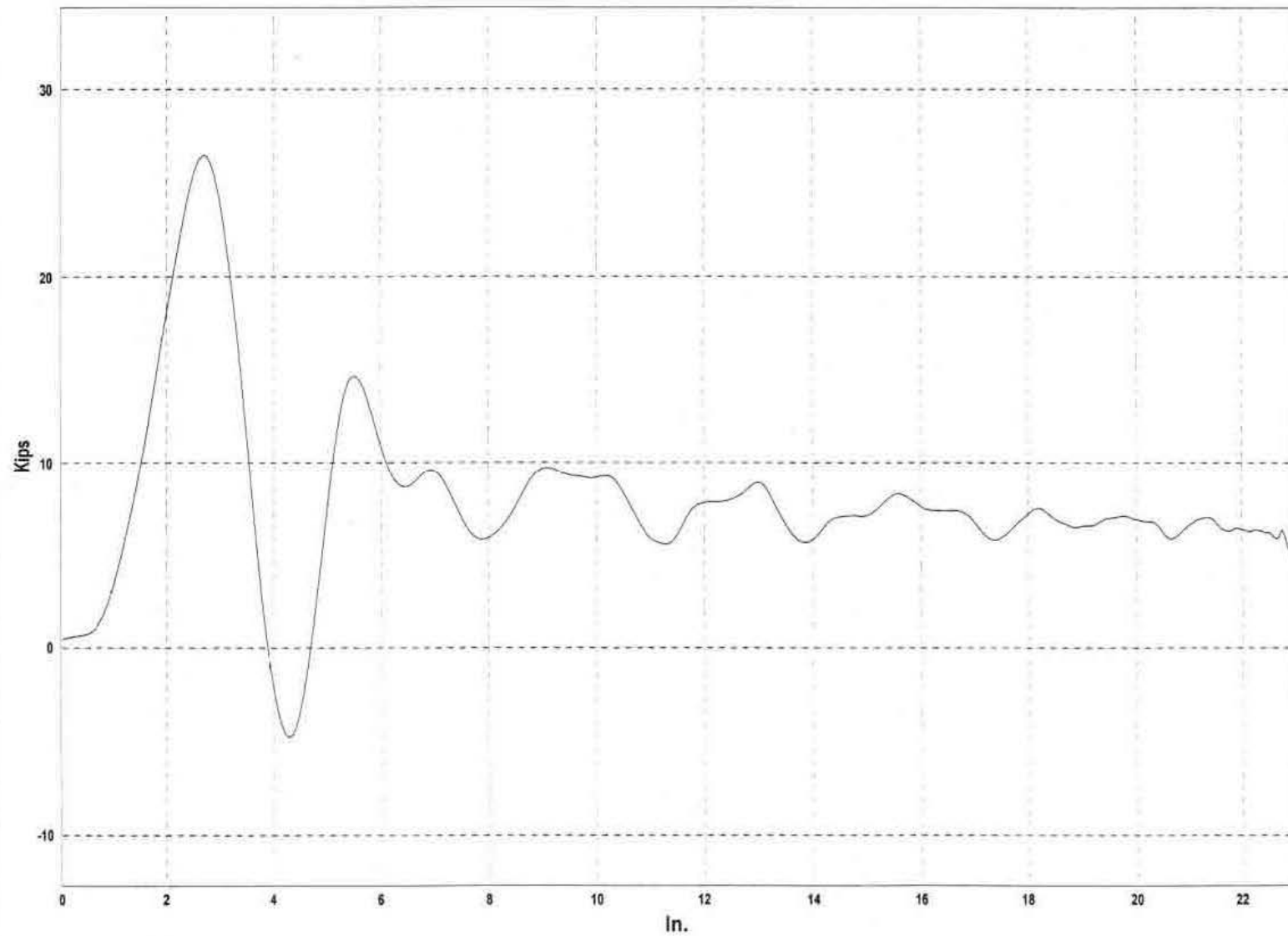


Figure A-1. Graph of Force-Deflection Behavior, Test MSB-1

W14: Force vs. Displacement - Test MSB-2

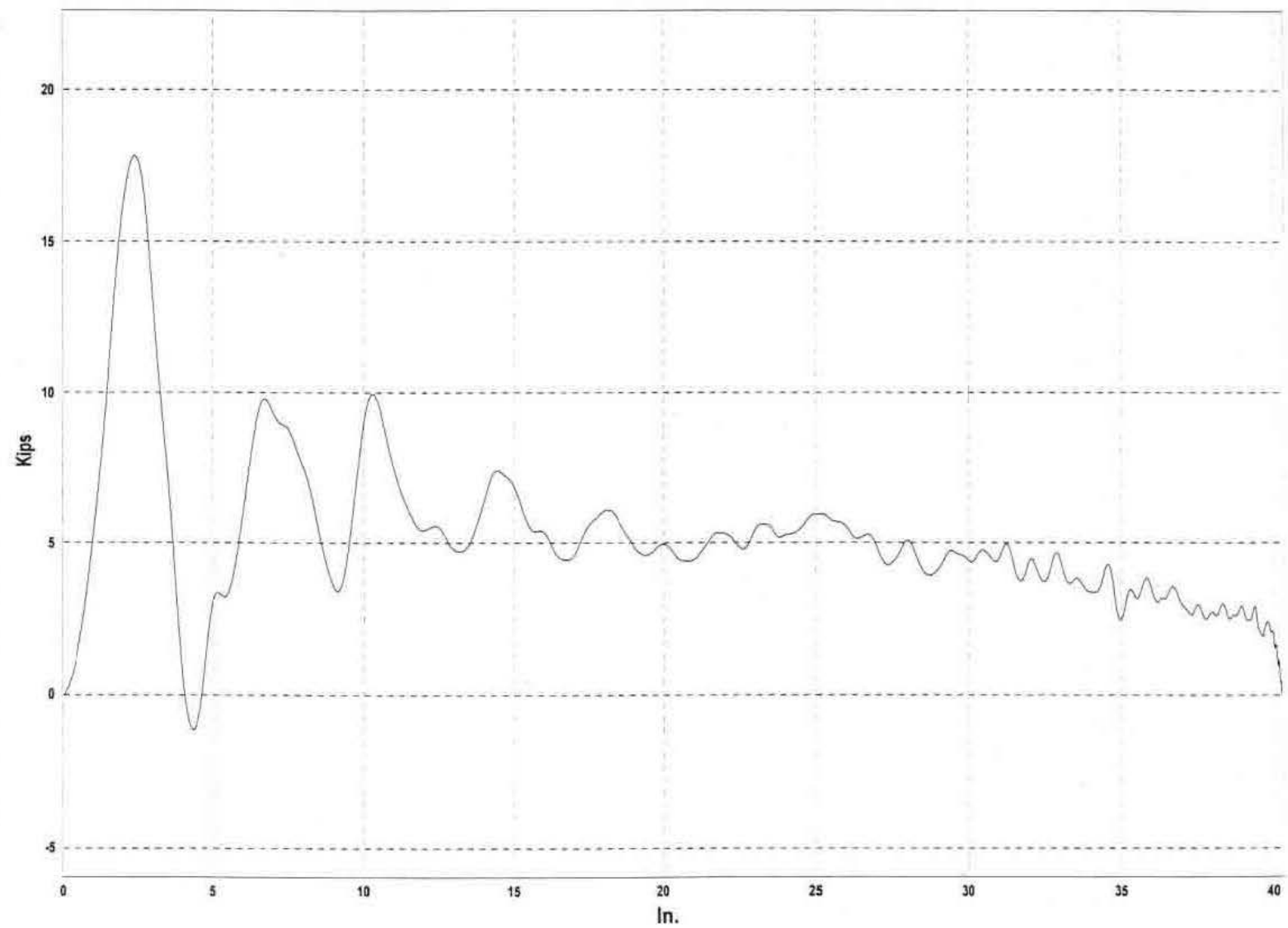


Figure A-2. Graph of Force-Deflection Behavior, Test MSB-2

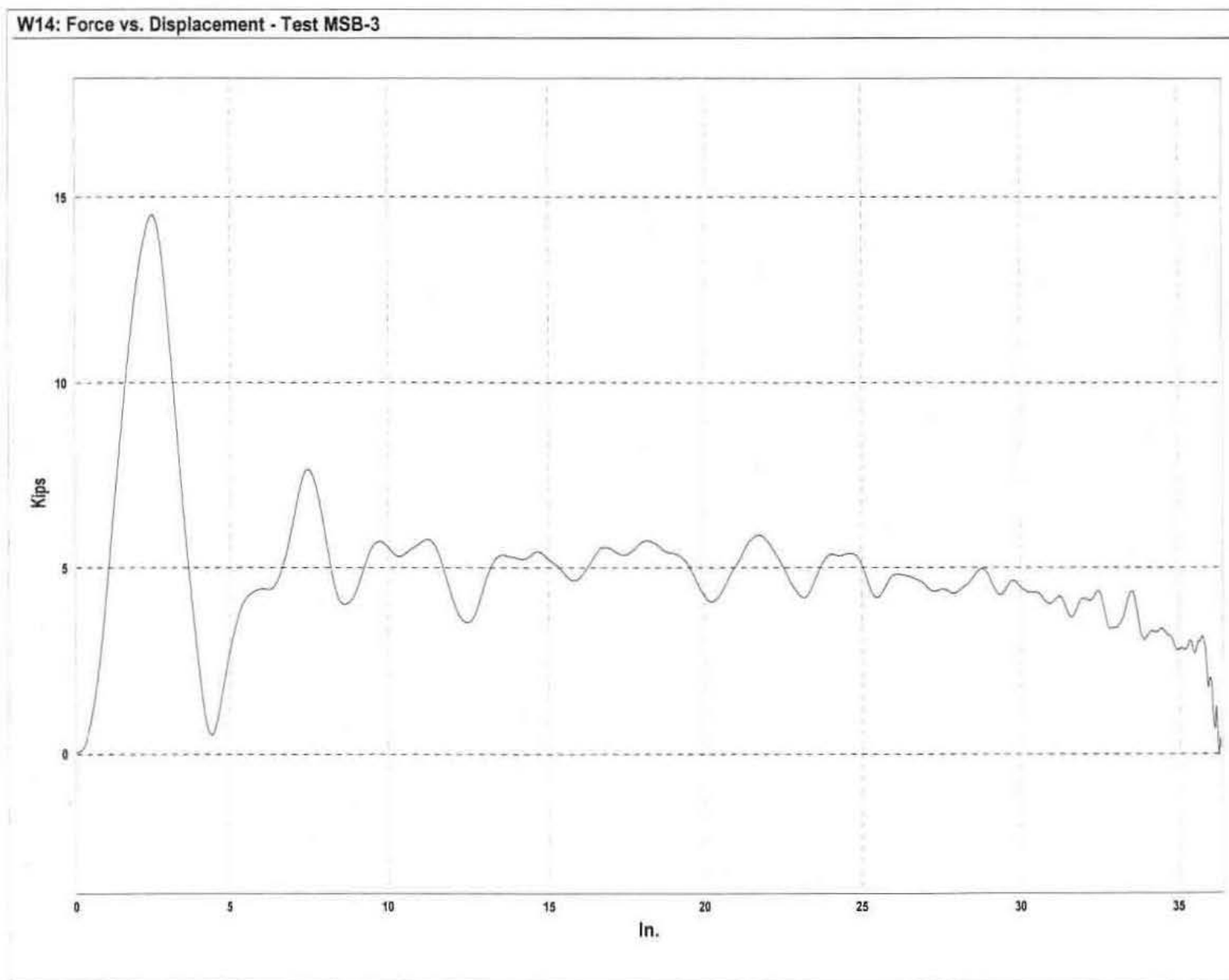


Figure A-3. Graph of Force-Deflection Behavior, Test MSB-3

W14: Force vs. Displacement - Test MSB-4

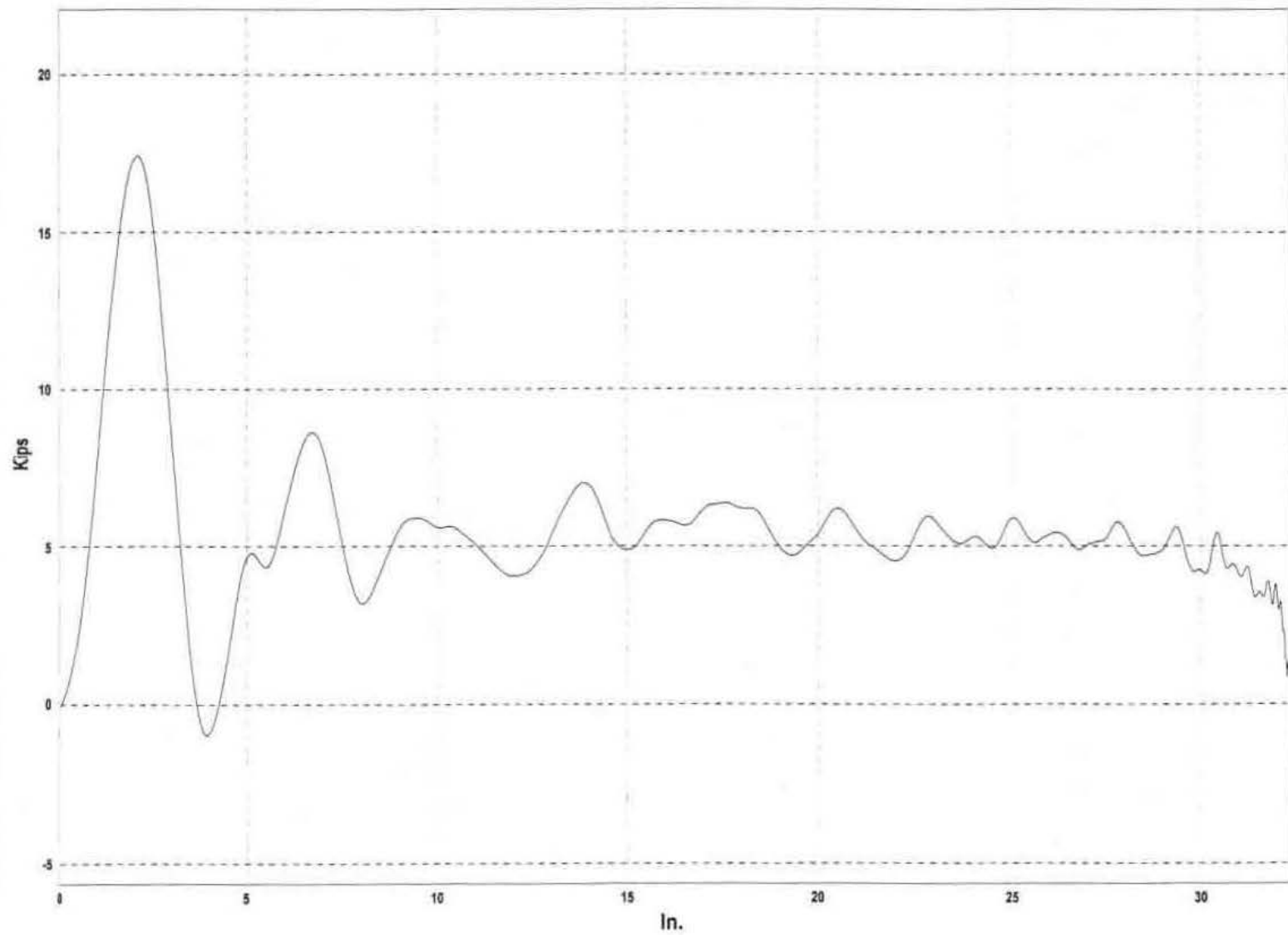


Figure A-4. Graph of Force-Deflection Behavior, Test MSB-4

W14: Force vs. Displacement - Test MSB-5

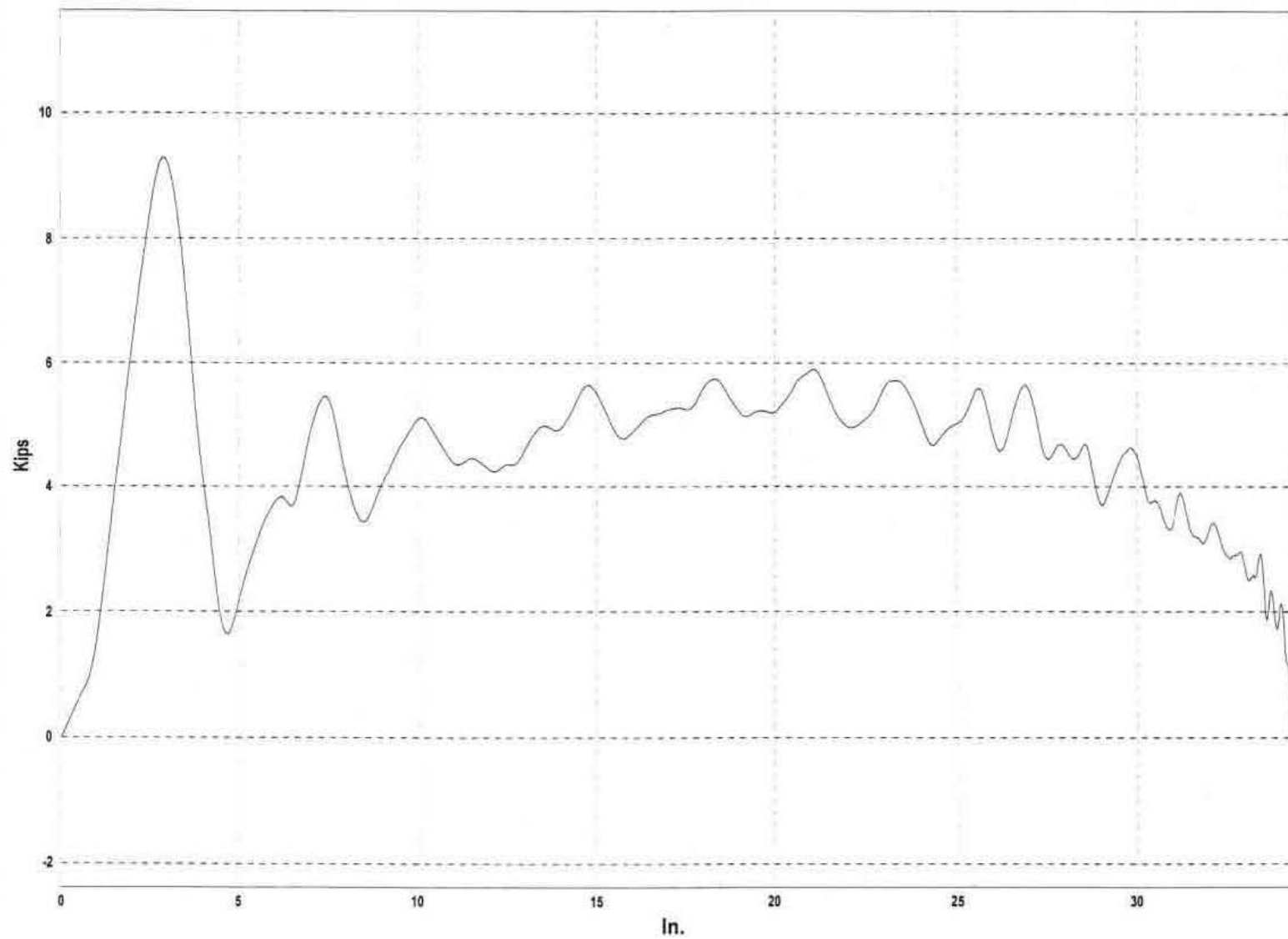


Figure A-5. Graph of Force-Deflection Behavior, Test MSB-5

W14: Force vs. Displacement - Test MSB-6

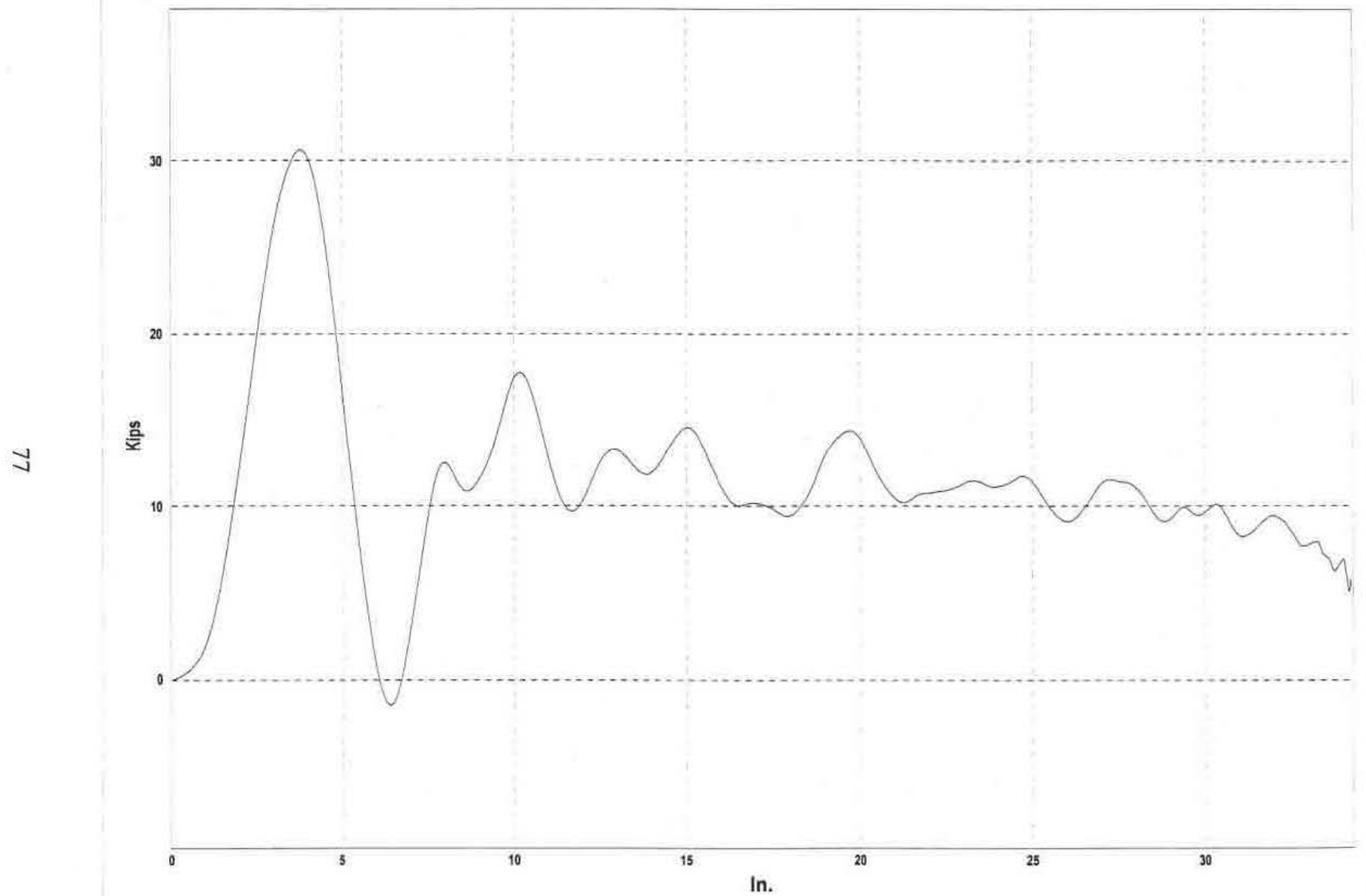


Figure A-6. Graph of Force-Deflection Behavior, Test MSB-6

APPENDIX B

Typical BARRIER VII Input File

Note that the example BARRIER VII input data file included in Appendix B corresponds with the critical impact point for test MOSW-1.

Missouri Guardrail Posts on Slopes (Half-Post Spacing) - RUN "Slope8DHPS.DAT" -
 NODE 83

173	71	28	1	213	85	2	0		
0.0001		0.0001			0.800	300	0	1.0	1
1	5	5	5	5	5	1			
1		0.0		0.0					
3		75.00		0.0					
5		150.00		0.0					
9		225.00		0.0					
12		281.25		0.0					
13		290.625		0.0					
14		295.3125		0.0					
15		300.00		0.0					
16		304.6875		0.0					
17		309.375		0.0					
18		318.75		0.0					
21		375.00		0.0					
25		450.00		0.0					
29		525.00		0.0					
32		581.25		0.0					
33		590.625		0.0					
34		595.3125		0.0					
35		600.00		0.0					
36		604.6875		0.0					
37		609.375		0.0					
38		618.75		0.0					
44		675.00		0.0					
52		750.00		0.0					
60		825.00		0.0					
66		881.25		0.0					
67		890.625		0.0					
68		895.3125		0.0					
69		900.00		0.0					
70		904.6875		0.0					
71		909.375		0.0					
72		918.75		0.0					
78		975.00		0.0					
84		1031.25		0.0					
85		1040.625		0.0					
86		1045.3125		0.0					
87		1050.00		0.0					
88		1054.6875		0.0					
89		1059.375		0.0					
90		1068.75		0.0					
96		1125.00		0.0					
102		1181.25		0.0					
103		1190.625		0.0					
104		1195.3125		0.0					
105		1200.00		0.0					
106		1204.6875		0.0					
107		1209.375		0.0					
108		1218.75		0.0					
114		1275.00		0.0					
122		1350.00		0.0					
130		1425.00		0.0					
136		1481.25		0.0					
137		1490.625		0.0					
138		1495.3125		0.0					
139		1500.00		0.0					

140	1504.6875			0.0					
141	1509.375			0.0					
142	1518.75			0.0					
145	1575.00			0.0					
149	1650.00			0.0					
153	1725.00			0.0					
156	1781.25			0.0					
157	1790.625			0.0					
158	1795.3125			0.0					
159	1800.00			0.0					
160	1804.6875			0.0					
161	1809.375			0.0					
162	1818.75			0.0					
165	1875.00			0.0					
169	1950.00			0.0					
171	2025.00			0.0					
173	2100.00			0.0					
1	3	1	1		0.0				
3	5	1	1		0.0				
5	9	3	1		0.0				
9	12	2	1		0.0				
18	21	2	1		0.0				
21	25	3	1		0.0				
25	29	3	1		0.0				
29	32	2	1		0.0				
38	44	5	1		0.0				
44	52	7	1		0.0				
52	60	7	1		0.0				
60	66	5	1		0.0				
72	78	5	1		0.0				
78	84	5	1		0.0				
90	96	5	1		0.0				
96	102	5	1		0.0				
108	114	5	1		0.0				
114	122	7	1		0.0				
122	130	7	1		0.0				
130	136	5	1		0.0				
142	145	2	1		0.0				
145	149	3	1		0.0				
149	153	3	1		0.0				
153	156	2	1		0.0				
162	165	2	1		0.0				
165	169	3	1		0.0				
169	171	1	1		0.0				
171	173	1	1		0.0				
1	173			0.35					
173	172	171	170	169	168	167	166	165	164
163	162	161	160	159	158	157	156	155	154
153	152	151	150	149	148	147	146	145	144
143	142	141	140	139	138	137	136	135	134
133	132	131	130	129	128	127	126	125	124
123	122	121	120	119	118	117	116	115	114
113	112	111	110	109	108	107	106	105	104
103	102	101	100	99	98	97	96	95	94
93	92	91	90	89	88	87	86	85	84
83	82	81	80	79	78	77	76	75	74
73	72	71	70	69	68	67	66	65	64
63	62	61	60	59	58	57	56	55	54
53	52	51	50	49	48	47	46	45	44

43	42	41	40	39	38	37	36	35	34										
33	32	31	30	29	28	27	26	25	24										
23	22	21	20	19	18	17	16	15	14										
13	12	11	10	9	8	7	6	5	4										
3	2	1																	
100	24																		
1	2.29		1.99		37.50		30000.0		6.92	99.5		68.5	0.10						
12-Gauge W-Beam																			
2	2.29		1.99		18.75		30000.0		6.92	99.5		68.5	0.10						
12-Gauge W-Beam																			
3	2.29		1.99		9.375		30000.0		6.92	99.5		68.5	0.10						
12-Gauge W-Beam																			
4	2.29		1.99		4.6875		30000.0		6.92	99.5		68.5	0.10						
12-Gauge W-Beam																			
5	2.29		1.99		4.6875		30000.0		6.92	99.5		68.5	0.10						
12-Gauge W-Beam																			
6	2.29		1.99		4.6875		30000.0		6.92	99.5		68.5	0.10						
12-Gauge W-Beam																			
7	2.29		1.99		4.6875		30000.0		6.92	99.5		68.5	0.10						
12-Gauge W-Beam																			
8	2.29		1.99		9.375		30000.0		6.92	99.5		68.5	0.10						
12-Gauge W-Beam																			
9	2.29		1.99		18.75		30000.0		6.92	99.5		68.5	0.10						
12-Gauge W-Beam																			
10	2.29		1.99		9.375		30000.0		6.92	99.5		68.5	0.10						
12-Gauge W-Beam																			
11	2.29		1.99		4.6875		30000.0		6.92	99.5		68.5	0.10						
12-Gauge W-Beam																			
12	2.29		1.99		4.6875		30000.0		6.92	99.5		68.5	0.10						
12-Gauge W-Beam																			
13	2.29		1.99		4.6875		30000.0		6.92	99.5		68.5	0.10						
12-Gauge W-Beam																			
14	2.29		1.99		4.6875		30000.0		6.92	99.5		68.5	0.10						
12-Gauge W-Beam																			
15	2.29		1.99		9.375		30000.0		6.92	99.5		68.5	0.10						
12-Gauge W-Beam																			
16	2.29		1.99		4.6875		30000.0		6.92	99.5		68.5	0.10						
12-Gauge W-Beam																			
17	2.29		1.99		4.6875		30000.0		6.92	99.5		68.5	0.10						
12-Gauge W-Beam																			
18	2.29		1.99		4.6875		30000.0		6.92	99.5		68.5	0.10						
12-Gauge W-Beam																			
19	2.29		1.99		4.6875		30000.0		6.92	99.5		68.5	0.10						
12-Gauge W-Beam																			
20	2.29		1.99		9.375		30000.0		6.92	99.5		68.5	0.10						
12-Gauge W-Beam																			
21	2.29		1.99		4.6875		30000.0		6.92	99.5		68.5	0.10						
12-Gauge W-Beam																			
22	2.29		1.99		4.6875		30000.0		6.92	99.5		68.5	0.10						
12-Gauge W-Beam																			
23	2.29		1.99		4.6875		30000.0		6.92	99.5		68.5	0.10						
12-Gauge W-Beam																			
24	2.29		1.99		4.6875		30000.0		6.92	99.5		68.5	0.10						
12-Gauge W-Beam																			
300	15																		
1	21.65		0.00		4.0		4.0		100.0	250.0		250.0	0.10						
Simulated Strong Anchor Post																			
100.0		100.0		10.0		10.0													
2	21.65		0.00		3.0		3.0		100.0	100.0		150.00	0.10						

Second BCT Post	50.0	50.0	6.0	6.0					
3 21.65	0.0	2.00	2.00	54.0	92.88	102.00	0.10		
W6x9 by 7' Long	6.0	15.0	15.0	15.0					
4 21.65	0.0	2.00	2.00	54.0	92.88	102.00	0.10		
W6x9 by 7' Long	6.0	15.0	15.0	15.0					
5 21.65	0.0	2.00	2.00	54.0	92.88	102.00	0.10		
W6x9 by 7' Long	6.0	15.0	15.0	15.0					
6 21.65	0.0	2.00	2.00	54.0	92.88	102.00	0.10		
W6x9 by 7' Long	6.0	15.0	15.0	15.0					
7 21.65	0.0	2.00	2.00	54.0	92.88	102.00	0.10		
W6x9 by 7' Long	6.0	15.0	15.0	15.0					
8 21.65	0.0	2.00	2.00	54.0	92.88	102.00	0.10		
W6x9 by 7' Long	6.0	15.0	15.0	15.0					
9 21.65	0.0	2.00	2.00	54.0	92.88	102.00	0.10		
W6x9 by 7' Long	6.0	15.0	15.0	15.0					
10 21.65	0.0	2.00	2.00	54.0	92.88	102.00	0.10		
W6x9 by 7' Long	6.0	15.0	15.0	15.0					
11 21.65	0.0	2.00	2.00	54.0	92.88	102.00	0.10		
W6x9 by 7' Long	6.0	15.0	15.0	15.0					
12 21.65	0.0	2.00	2.00	54.0	92.88	102.00	0.10		
W6x9 by 7' Long	6.0	15.0	15.0	15.0					
13 21.65	0.0	2.00	2.00	54.0	92.88	102.00	0.10		
W6x9 by 7' Long	6.0	15.0	15.0	15.0					
14 21.65	0.0	2.00	2.00	54.0	92.88	102.00	0.10		
W6x9 by 7' Long	6.0	15.0	15.0	15.0					
15 21.65	0.0	2.00	2.00	54.0	92.88	102.00	0.10		
W6x9 by 7' Long	6.0	15.0	15.0	15.0					
(Half-Post Spacing)	15.0	15.0	15.0						
1 1 2 4 1 101	0.0	0.0	0.0						
5 5 6 11 1 102	0.0	0.0	0.0						
12 12 13 103	0.0	0.0	0.0						
13 13 14 104	0.0	0.0	0.0						
14 14 15 105	0.0	0.0	0.0						
15 15 16 106	0.0	0.0	0.0						
16 16 17 107	0.0	0.0	0.0						
17 17 18 108	0.0	0.0	0.0						
18 18 19 31 1 109	0.0	0.0	0.0						
32 32 33 110	0.0	0.0	0.0						
33 33 34 111	0.0	0.0	0.0						
34 34 35 112	0.0	0.0	0.0						
35 35 36 113	0.0	0.0	0.0						
36 36 37 114	0.0	0.0	0.0						
37 37 38 66 1 115	0.0	0.0	0.0						
67 67 68 116	0.0	0.0	0.0						
68 68 69 117	0.0	0.0	0.0						
69 69 70 118	0.0	0.0	0.0						

70	70	71			119	0.0	0.0	0.0		
71	71	72	84	1	120	0.0	0.0	0.0		
85	85	86			121	0.0	0.0	0.0		
86	86	87			122	0.0	0.0	0.0		
87	87	88			123	0.0	0.0	0.0		
88	88	89			124	0.0	0.0	0.0		
89	89	90	102	1	120	0.0	0.0	0.0		
103	103	104			119	0.0	0.0	0.0		
104	104	105			118	0.0	0.0	0.0		
105	105	106			117	0.0	0.0	0.0		
106	106	107			116	0.0	0.0	0.0		
107	107	108	136	1	115	0.0	0.0	0.0		
137	137	138			114	0.0	0.0	0.0		
138	138	139			113	0.0	0.0	0.0		
139	139	140			112	0.0	0.0	0.0		
140	140	141			111	0.0	0.0	0.0		
141	141	142			110	0.0	0.0	0.0		
142	142	143	155	1	109	0.0	0.0	0.0		
156	156	157			108	0.0	0.0	0.0		
157	157	158			107	0.0	0.0	0.0		
158	158	159			106	0.0	0.0	0.0		
159	159	160			105	0.0	0.0	0.0		
160	160	161			104	0.0	0.0	0.0		
161	161	162			103	0.0	0.0	0.0		
162	162	163	168	1	102	0.0	0.0	0.0		
169	169	170	172	1	101	0.0	0.0	0.0		
173	1				301	0.0	0.0	0.0	0.0	0.0
174	3				302	0.0	0.0	0.0	0.0	0.0
175	5				303	0.0	0.0	0.0	0.0	0.0
176	9				303	0.0	0.0	0.0	0.0	0.0
177	15				303	0.0	0.0	0.0	0.0	0.0
178	21				303	0.0	0.0	0.0	0.0	0.0
179	25				303	0.0	0.0	0.0	0.0	0.0
180	29				303	0.0	0.0	0.0	0.0	0.0
181	35				303	0.0	0.0	0.0	0.0	0.0
182	44				304	0.0	0.0	0.0	0.0	0.0
183	52				305	0.0	0.0	0.0	0.0	0.0
184	60				306	0.0	0.0	0.0	0.0	0.0
185	69				307	0.0	0.0	0.0	0.0	0.0
186	78				308	0.0	0.0	0.0	0.0	0.0
187	87				309	0.0	0.0	0.0	0.0	0.0
188	96				310	0.0	0.0	0.0	0.0	0.0
189	105				311	0.0	0.0	0.0	0.0	0.0
190	114				312	0.0	0.0	0.0	0.0	0.0
191	122				313	0.0	0.0	0.0	0.0	0.0
192	130				314	0.0	0.0	0.0	0.0	0.0
193	139				303	0.0	0.0	0.0	0.0	0.0
194	145				303	0.0	0.0	0.0	0.0	0.0
195	149				303	0.0	0.0	0.0	0.0	0.0
196	153				303	0.0	0.0	0.0	0.0	0.0
197	159				303	0.0	0.0	0.0	0.0	0.0
198	165				303	0.0	0.0	0.0	0.0	0.0
199	169				303	0.0	0.0	0.0	0.0	0.0
200	171				302	0.0	0.0	0.0	0.0	0.0
201	173				301	0.0	0.0	0.0	0.0	0.0
202	40				315	0.0	0.0	0.0	0.0	0.0
203	48				315	0.0	0.0	0.0	0.0	0.0
204	56				315	0.0	0.0	0.0	0.0	0.0
205	64				315	0.0	0.0	0.0	0.0	0.0

206	74		315	0.0	0.0	0.0	0.0	0.0
207	82		315	0.0	0.0	0.0	0.0	0.0
208	92		315	0.0	0.0	0.0	0.0	0.0
209	100		315	0.0	0.0	0.0	0.0	0.0
210	110		315	0.0	0.0	0.0	0.0	0.0
211	118		315	0.0	0.0	0.0	0.0	0.0
212	126		315	0.0	0.0	0.0	0.0	0.0
213	134		315	0.0	0.0	0.0	0.0	0.0
	4400.0	40000.0	20	6	4	0	1	
1	0.055	0.12		6.00			17.0	
2	0.057	0.15		7.00			18.0	
3	0.062	0.18		10.00			12.0	
4	0.110	0.35		12.00			6.0	
5	0.35	0.45		6.00			5.0	
6	1.45	1.50		15.00			1.0	
1	100.75	15.875	1	12.0	1	1	0	0
2	100.75	27.875	1	12.0	1	1	0	0
3	100.75	39.875	2	12.0	1	1	0	0
4	88.75	39.875	2	12.0	1	1	0	0
5	76.75	39.875	2	12.0	1	1	0	0
6	64.75	39.875	2	12.0	1	1	0	0
7	52.75	39.875	2	12.0	1	1	0	0
8	40.75	39.875	2	12.0	1	1	0	0
9	28.75	39.875	2	12.0	1	1	0	0
10	16.75	39.875	2	12.0	1	1	0	0
11	-13.25	39.875	3	12.0	1	1	0	0
12	-33.25	39.875	3	12.0	1	1	0	0
13	-53.25	39.875	3	12.0	1	1	0	0
14	-73.25	39.875	3	12.0	1	1	0	0
15	-93.25	39.875	3	12.0	1	1	0	0
16	-113.25	39.875	4	12.0	1	1	0	0
17	-113.25	-39.875	4	12.0	0	0	0	0
18	100.75	-39.875	1	12.0	0	0	0	0
19	69.25	37.75	5	1.0	1	1	0	0
20	-62.75	37.75	6	1.0	1	1	0	0
1	69.25	32.75		0.0			608.	
2	69.25	-32.75		0.0			608.	
3	-62.75	32.75		0.0			492.	
4	-62.75	-32.75		0.0			492.	
1	0.0	0.0						
3	1021.875	0.0		25.0	62.14	0.0	0.0	1.0

APPENDIX C

Accelerometer Data Analysis, Test MOSW-1

Figure C-1. Graph of Longitudinal Deceleration, Test MOSW-1

Figure C-2. Graph of Longitudinal Occupant Impact Velocity, Test MOSW-1

Figure C-3. Graph of Longitudinal Occupant Displacement, Test MOSW-1

Figure C-4. Graph of Lateral Deceleration, Test MOSW-1

Figure C-5. Graph of Lateral Occupant Impact Velocity, Test MOSW-1

Figure C-6. Graph of Lateral Occupant Displacement, Test MOSW-1

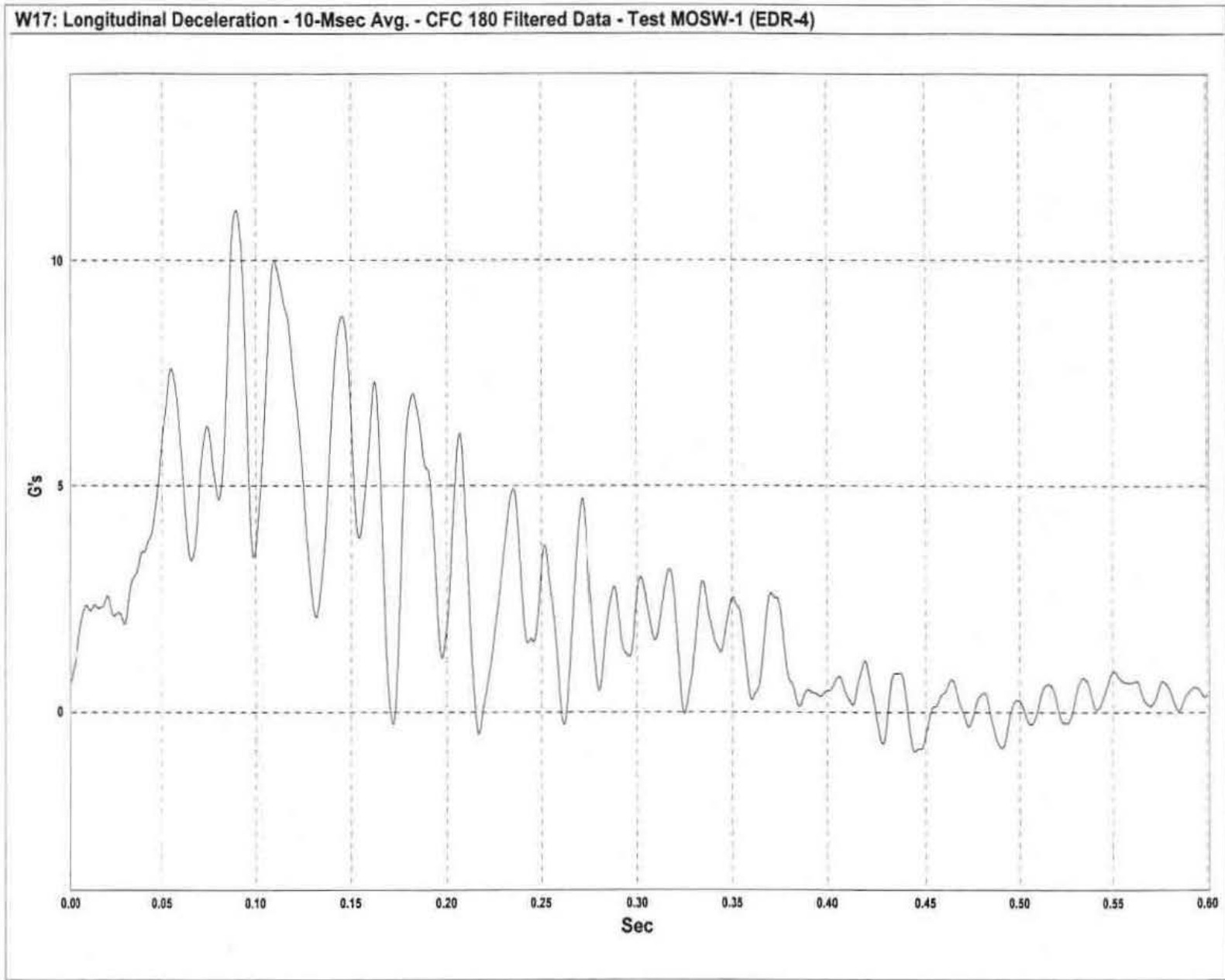


Figure C-1. Graph of Longitudinal Deceleration, Test MOSW-1

W8: Longitudinal Occupant Impact Velocity - CFC 180 Filtered Data - Test MOSW-1 (EDR-4)

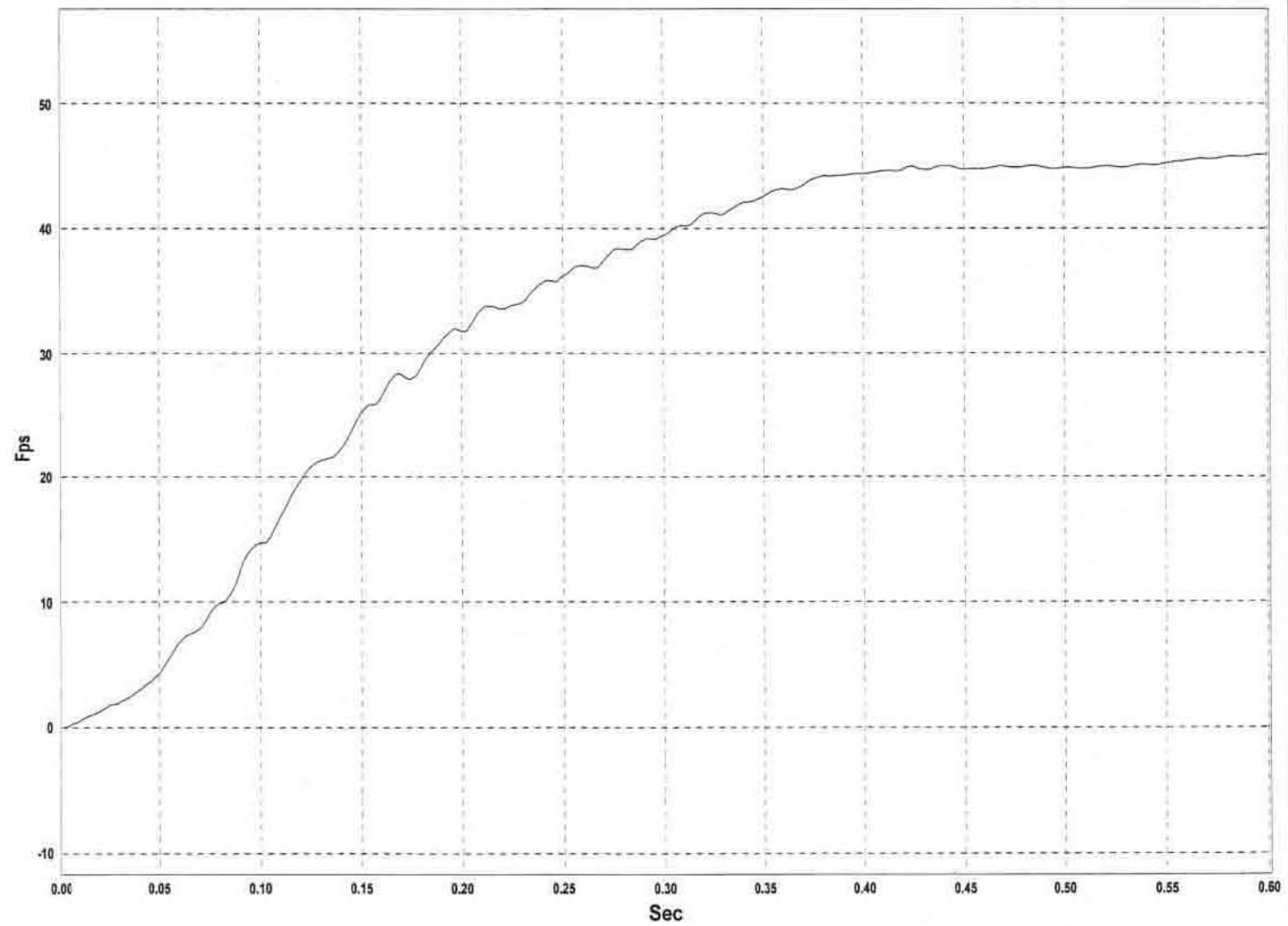


Figure C-2. Graph of Longitudinal Occupant Impact Velocity, Test MOSW-1

W9: Longitudinal Occupant Displacement - CFC 180 Filtered Data - Test MOSW-1 (EDR-4)

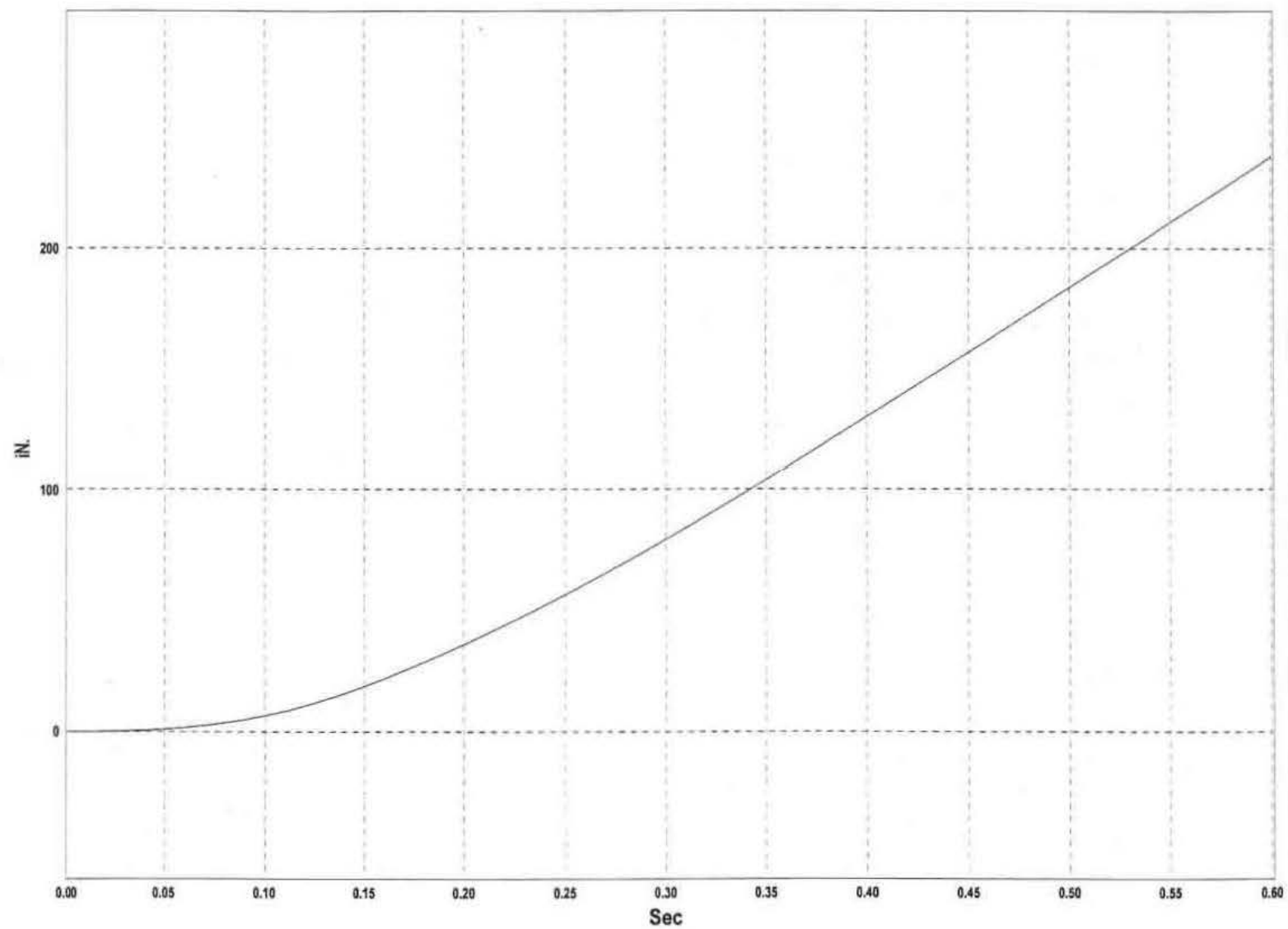


Figure C-3. Graph of Longitudinal Occupant Displacement, Test MOSW-1

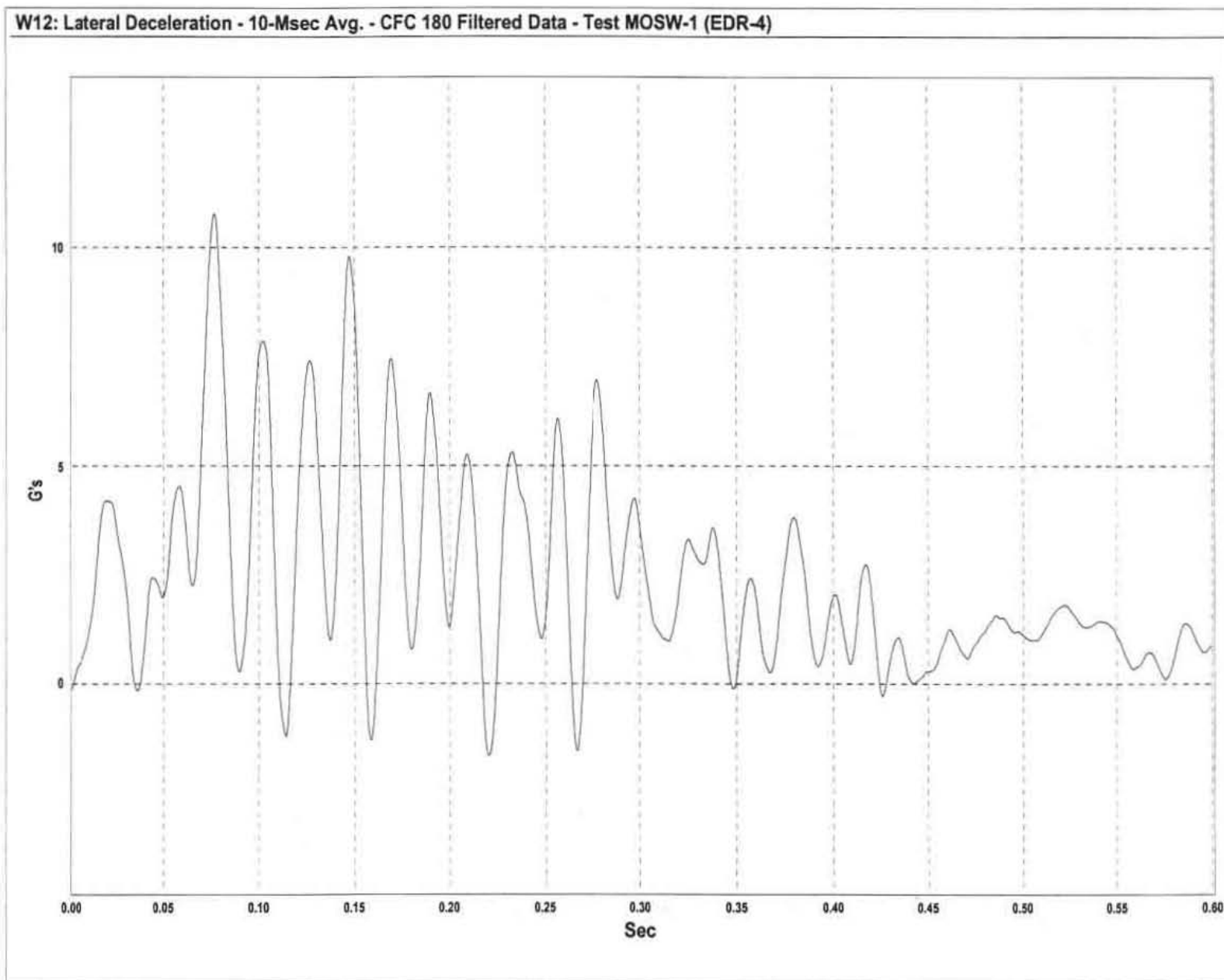


Figure C-4. Graph of Lateral Deceleration, Test MOSW-1

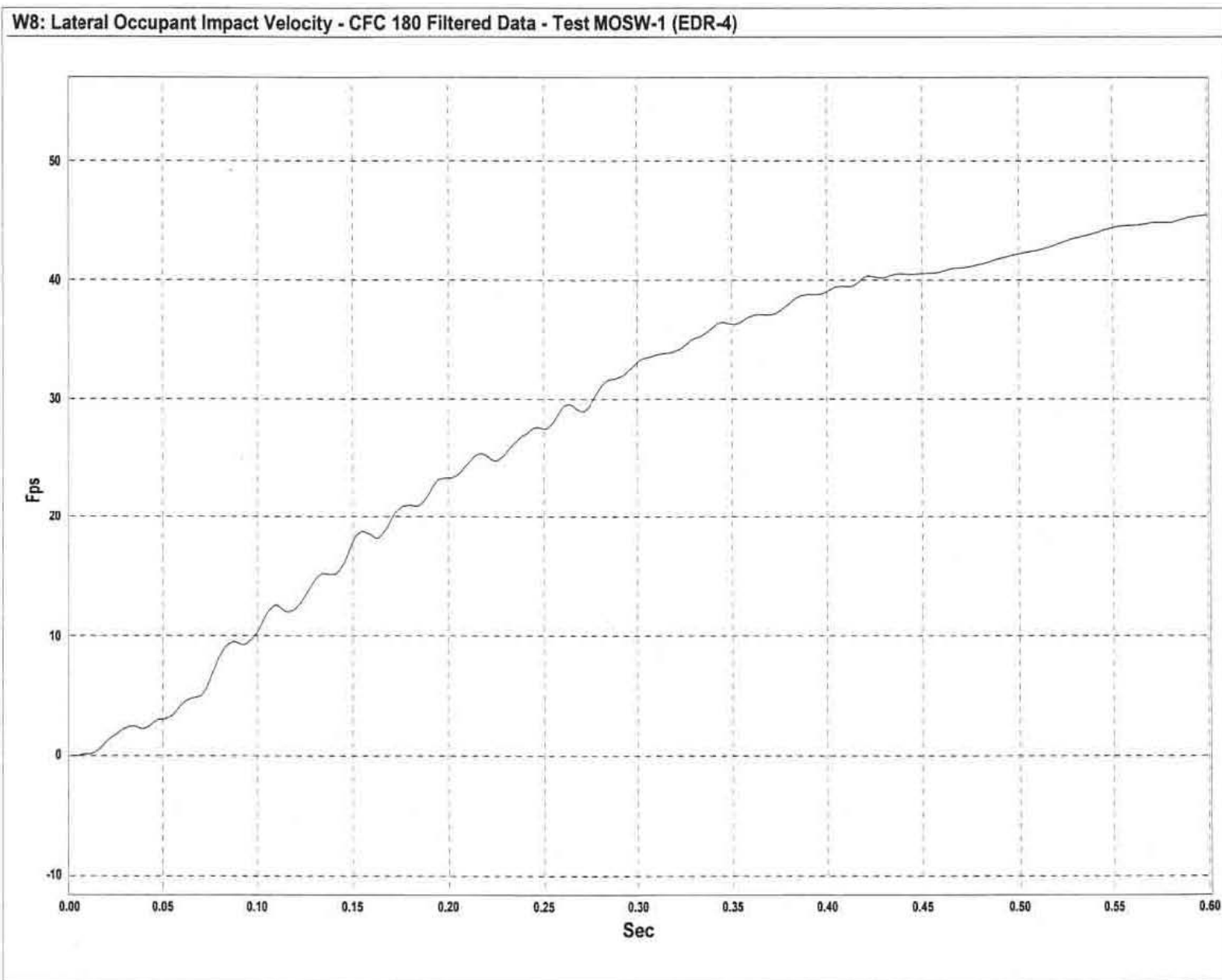


Figure C-5. Graph of Lateral Occupant Impact Velocity, Test MOSW-1

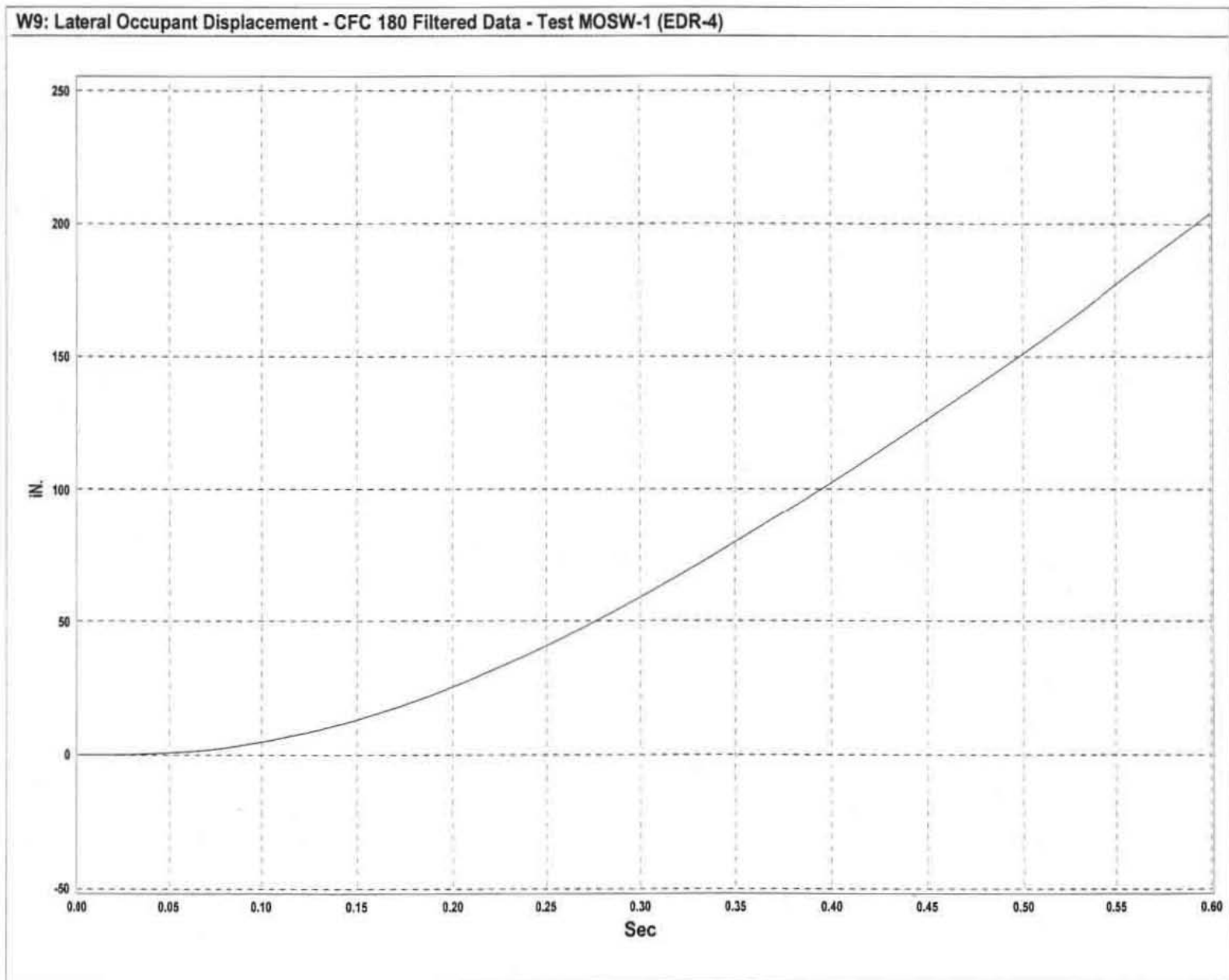


Figure C-6. Graph of Lateral Occupant Displacement, Test MOSW-1

APPENDIX D

Roll, Pitch, and Yaw Data Analysis, Test MOSW-1

Figure D-1. Graph of Roll Angular Displacements, Test MOSW-1

Figure D-2. Graph of Pitch Angular Displacements, Test MOSW-1

Figure D-3. Graph of Yaw Angular Displacements, Test MOSW-1

Missouri Guardrail On Slope

MOSW-1, Roll Angle

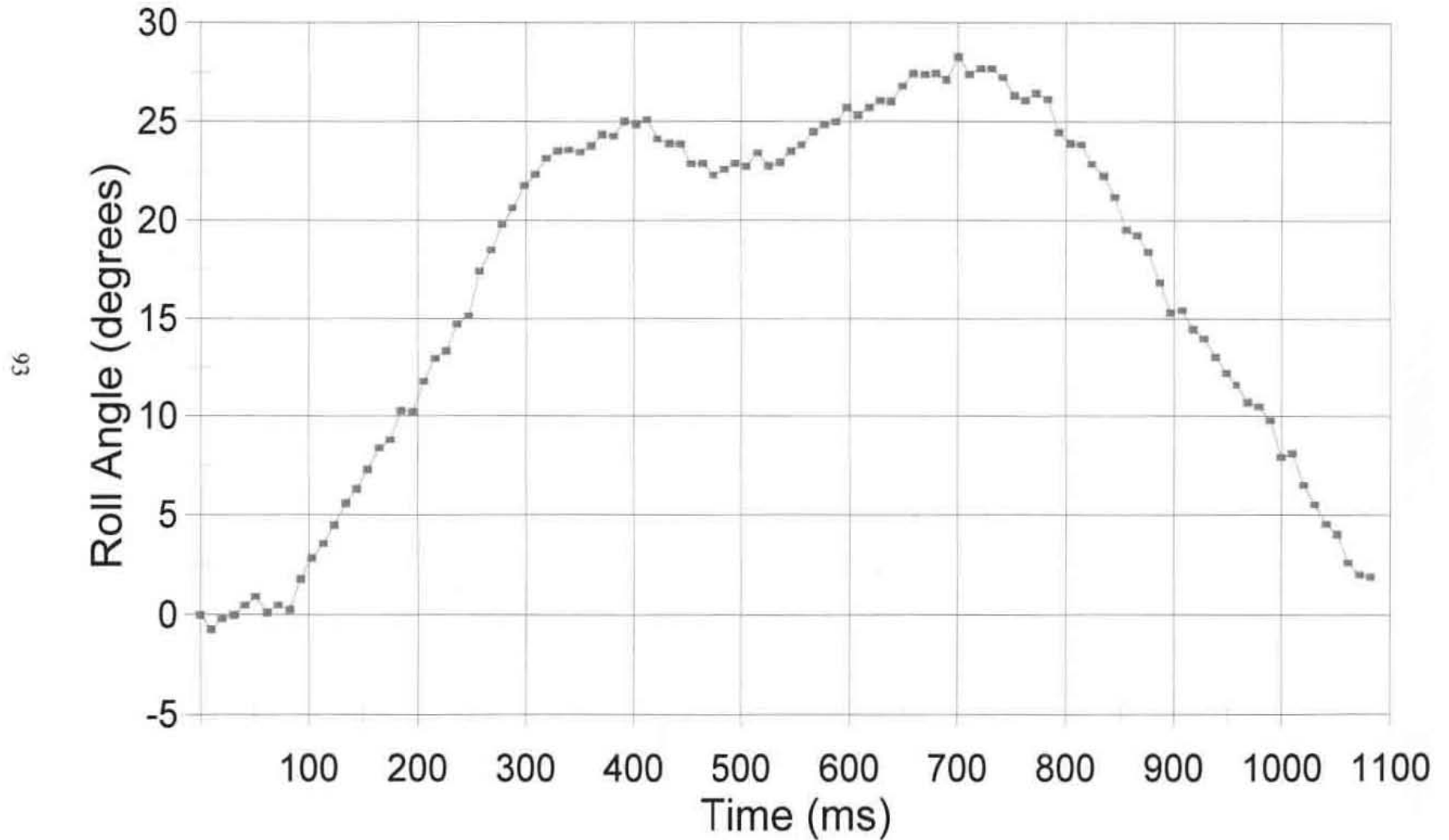


Figure D-1. Graph of Roll Angular Displacements, Test MOSW-1

Missouri Guardrail On Slope

MOSW-1, Pitch Angle

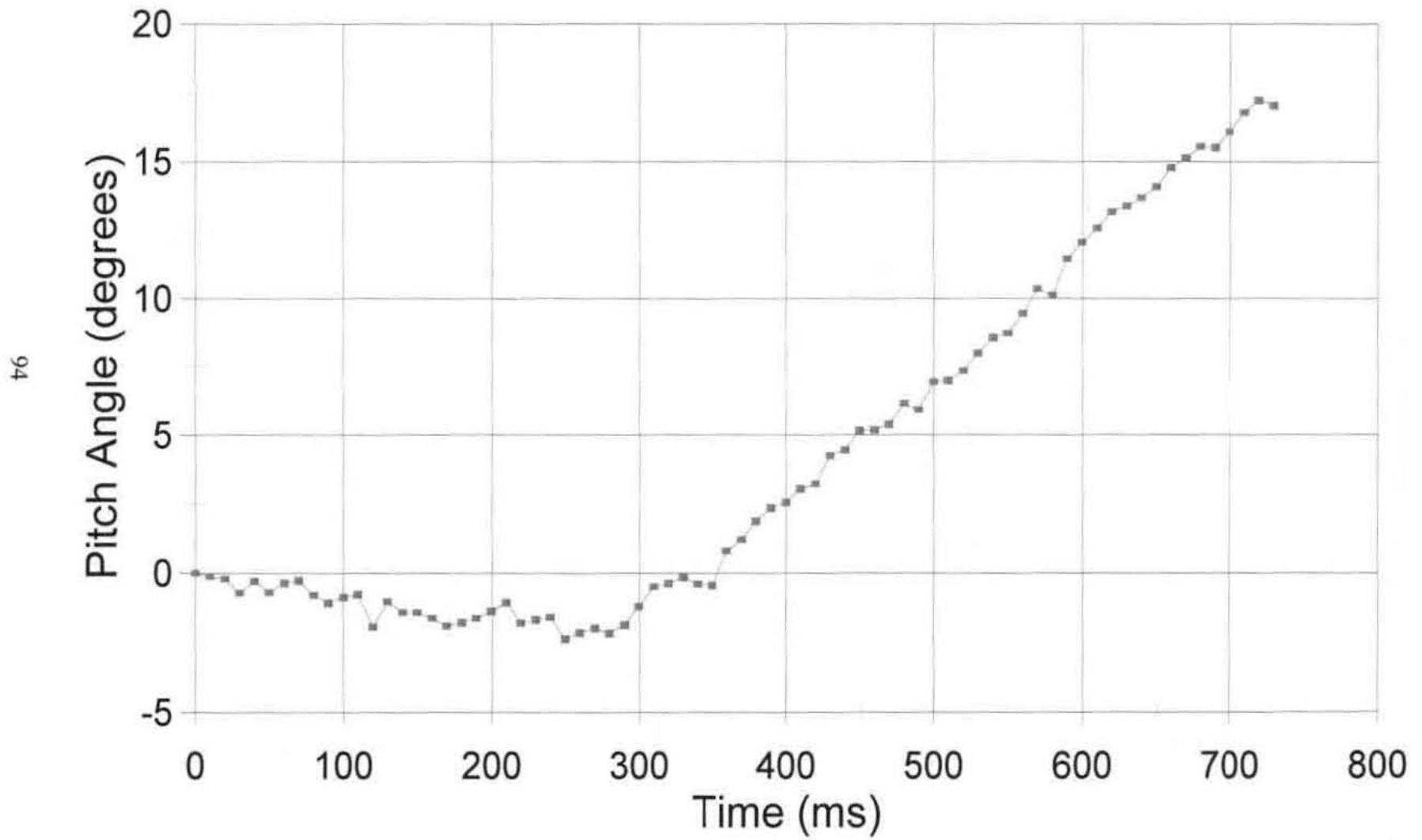


Figure D-2. Graph of Pitch Angular Displacements, Test MOSW-1

Missouri Guardrail On Slope

MOSW-1, Yaw Angle

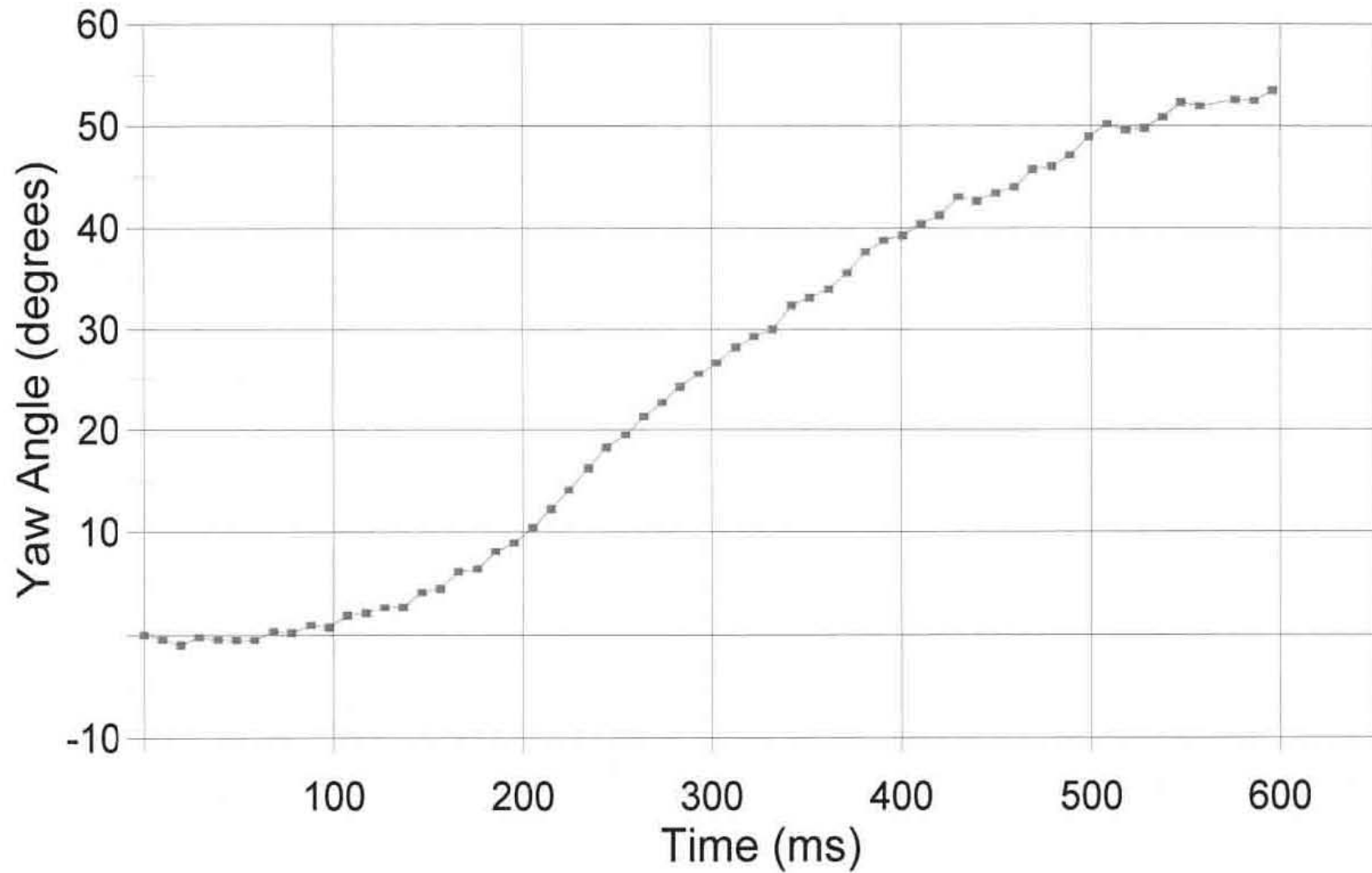


Figure D-3. Graph of Yaw Angular Displacements, Test MOSW-1